LLM-TS Integrator: Integrating LLM for Enhanced Time Series Modeling

Anonymous authors
Paper under double-blind review

Abstract

Time series (TS) modeling is essential in dynamic systems like weather prediction and anomaly detection. Recent studies utilize Large Language Models (LLMs) for TS modeling, leveraging their powerful pattern recognition capabilities. These methods primarily position LLMs as the predictive backbone, often omitting the mathematical modeling within traditional TS models, such as periodicity. However, disregarding the potential of LLMs also overlooks their pattern recognition capabilities. To address this gap, we introduce *LLM-TS Integrator*, a novel framework that effectively integrates the capabilities of LLMs into traditional TS modeling. Central to this integration is our *mutual information* module. The core of this *mutual information* module is a traditional TS model enhanced with LLM-derived insights for improved predictive abilities. This enhancement is achieved by maximizing the mutual information between traditional model's TS representations and LLM's textual representation counterparts, bridging the two modalities. Moreover, we recognize that samples vary in importance for two losses: traditional prediction and mutual information maximization. To address this variability, we introduce the *sample reweighting* module to improve information utilization. This module assigns dual weights to each sample: one for prediction loss and another for mutual information loss, dynamically optimizing these weights via bi-level optimization. Our method achieves state-of-the-art or comparable performance across five mainstream TS tasks, including short-term and long-term forecasting, imputation, classification, and anomaly detection. Our code is available at: `https://anonymous.4open.science/r/llm_ts_anonymous-F07D/README.MD`

1 Introduction

Time series (TS) modeling, as emphasized in Hyndman and Athanasopoulos (2018), is crucial for a variety of real-world applications. It is instrumental in forecasting meteorological factors for weather prediction (Wu et al., 2021), imputing missing data in economic TS (Friedman, 1962), detecting anomalies in industrial monitoring data for maintenance (Gao et al., 2020), and classifying trajectories for action recognition (Franceschi et al., 2019). Given its significant practical impact, TS analysis continues to attract substantial attention (Lim and Zohren, 2021; Wen et al., 2022).

Recent efforts in TS modeling have increasingly adopted Large Language Models (LLMs) to leverage their exceptional pattern recognition capabilities (Jiang et al., 2024; Zhou et al., 2023; Jin et al., 2024; Sun et al., 2023; Gruver et al., 2023b; Cao et al., 2024). While these innovative approaches validate the potential of LLMs in TS modeling, they primarily position LLMs as the core predictive model. Consequently, they often omit the mathematical modeling tailored specifically for TS models, such as employing the Fourier Transform to capture periodic patterns (Wu et al., 2023).

On the other hand, fully disregarding the potential of LLMs also overlooks their powerful pattern recognition capabilities. It is important to recognize the balance between leveraging LLMs for their advanced capabilities and utilizing traditional TS models for their mathematical modeling, to enhance the overall performance and accuracy of TS predictions. In response, we propose *LLM-TS Integrator*, a novel framework that effectively integrates the capabilities of LLMs into traditional TS modeling.

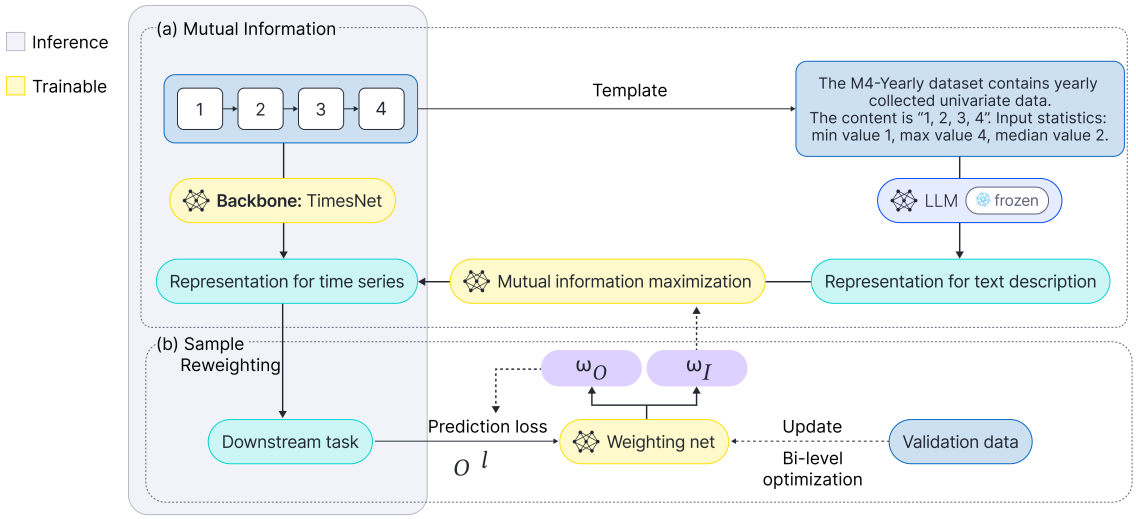

Figure 1: Illustration of *LLM-TS Integrator*. Module (a) enhances the traditional TS model (TimesNet) with LLM-derived insights by mutual information maximization. Module (b) optimizes sample importance for both prediction loss and mutual information loss to improve information utilization. The LLM is utilized solely during the training phase and is not required during inference.

Central to our framework is a *mutual information* module, as depicted in Figure 1(a). The core of this module is a traditional predictive model, which we enhance with insights derived from LLMs to improve its predictive abilities. In this work, we primarily utilize TimesNet (Wu et al., 2023) as the traditional predictive model due to its exceptional performance and insight into periodic modeling, and our framework is also applicable to other traditional TS models (see in Section 4.6.3). We achieve this enhancement by maximizing the mutual information (Sun et al., 2020) between the TS representations from traditional models and their textual counterparts from LLMs, thereby bridging these two modalities (a detailed discussion of various LLMs is provided in Section 4.6.4). Despite its established use, mutual information maximization has not been previously applied to the intersection of TS and text domain. With textual descriptions often missing from TS data, we propose generating such descriptions via a carefully designed template. This template is enriched with essential background and statistical details pertinent to the TS, thereby enriching the LLM's comprehension of the TS context (a comprehensive discussion of various templates is in Appendix A.5).

Our first module introduces a dual loss framework: traditional prediction and mutual information, and we recognize that the importance of samples differs between the two losses. For instance, a large prediction loss for a sample highlights its learning potential, emphasizing the need to focus on its prediction loss. This scenario also implies that the model's learning for this sample is inadequate and its hidden representation is suboptimal for mutual information computation. Consequently, the sample's contribution to the mutual information calculation should be reduced. To manage this variability, we have introduced a novel *sample reweighting* module powered by a simple MLP (multilayer perceptron) network, as depicted in Figure 1(b). This module processes the sample prediction loss to produce dual weights for each sample, one for the prediction loss and another for the mutual information loss. These weights are optimized through bi-level optimization, thereby enhancing the efficacy of information utilization.

Our primary contributions are as follows:

- We introduce the *LLM-TS Integrator* framework, which consists of *mutual information* and *sample reweighting*. The first module enhances traditional TS modeling with capabilities from LLMs through mutual information maximization.
- The second module optimizes sample importance for both prediction loss and mutual information loss, which improves information utilization.

- Extensive experiments across five mainstream TS tasks—short-term and long-term forecasting, imputation, classification, and anomaly detection—demonstrate the effectiveness of our framework. Obtained experimental results align across state-of-the-art of traditional time series and various LLMs which demonstrates applicability of *LLM-TS Integrator* framework regardless of choice of methods.
- *LLM-TS Integrator* framework keeps LLMs frozen and does not require fine-tuning and introduces minimum additional costs compared to traditional time series methods.

2 Preliminaries

TimesNet. In this paper, we mainly choose TimesNet as the traditional predictive model due to its exceptional performance (Wu et al., 2023) and also explore other additional traditional models including ETSformer (Woo et al., 2022), Stationary (Liu et al., 2022b), and FreTS (Yi et al., 2023) in Section 4.6. Previous studies to modeling temporal variations in 1D time series often struggle with complex temporal patterns. TimesNet addresses this challenge by decomposing these complex variations into multiple intra-period and inter-period variations. This is achieved by transforming the 1D time series into a series of 2D tensors, each corresponding to different periods. For the time series $\boldsymbol{x}$, we derive its representation $\boldsymbol{h}_{\boldsymbol{\theta}}^{m}(\boldsymbol{x})$ using the TimesNet model parameterized by $\boldsymbol{\theta}$ where m represents *model*.

Large Language Models. Language models are trained on extensive collections of natural language sequences, with each sequence consisting of multiple tokens. Notable large language models such as GPT-3 (Brown et al., 2020) and Llama2 (Touvron et al., 2023) aim to predict the next token based on preceding tokens, demonstrating their capabilities through improvements in model parameter size and the amount of training data. Each language model uses a tokenizer that breaks down an input string into a sequence of recognizable tokens. However, the training of current large language models is solely focused on natural language, not encompassing time series data. This limitation presents challenges for the direct application of large language models to time series analysis.

3 Method

In this section, we present the *LLM-TS Integrator* framework, which effectively integrates the capabilities of LLMs into traditional TS modeling. This framework consists of two modules: *mutual information* and *sample reweighting*. The first module enhances a traditional TS model with LLM-derived insights for improved predictive abilities, as explored in Section 3.1. The second module optimizes weights for prediction loss and mutual information loss via bi-level optimization, improving information utilization, as covered in Section 3.2. The overall algorithm is shown in Algorithm 1.

3.1 Mutual Information

Previous studies (Zhou et al., 2023; Jin et al., 2023) have predominantly highlighted the use of Large Language Models (LLMs) as the core predictive model in the TS analysis, often omitting the mathematical modeling within traditional TS models, such as periodicity.

In contrast, our framework utilizes a traditional TS model as the predictive backbone, enhanced by the advanced capabilities of LLMs. In this paper, we employ TimesNet, as outlined in Section 2, as the traditional predictive model, and we further examine other models in Section 4.6. This hybrid methodology combines the advantages of both traditional TS models and modern LLMs. We achieve this integration via a *mutual information* module, which maximizes the mutual information between the TS data representations derived from the traditional model and their corresponding textual representations derived from LLMs.

3.1.1 Mutual Information Estimation.

Estimating the mutual information between hidden representations of a time series (TS) sample $\boldsymbol{x}$ and its corresponding textual description $\boldsymbol{t}$ is essential. For the TS sample $\boldsymbol{x}$, we derive its representation $\boldsymbol{h}_{\boldsymbol{\theta}}^{m}(\boldsymbol{x})$ using TimesNet, a **m**odel parameterized by $\boldsymbol{\theta}$. For the text $\boldsymbol{t}$, its representation $\boldsymbol{h}^{l}(\boldsymbol{t})$ is extracted using a pre-trained

Algorithm 1 LLM-TS Integrator

Input: The TS dataset $\mathcal{D}$, number of training iterations T.
Output: Trained TS model parameterized by $\boldsymbol{\theta}^*$.

1: */* Mutual Information Module */*
2: Train a traditional TS model (e.g., TimesNet) parameterized by $\boldsymbol{\theta}$ using $\mathcal{D}$.
3: Generate text description $\boldsymbol{t}$ for TS sample $\boldsymbol{x}$ via a designed template.
4: Derive hidden representations $\boldsymbol{h}^m_{\boldsymbol{\theta}}(\boldsymbol{x})$ from the TS model and $\boldsymbol{h}^l(\boldsymbol{t})$ from the LLM.
5: **while** $\tau <= T-1$ **do**
6: Sample $\boldsymbol{x}$, $\boldsymbol{t}$, $\boldsymbol{y}$ from $\mathcal{D}$, where $\boldsymbol{y}$ are the labels.
7: Optimize a discriminator model $T_{\boldsymbol{\beta}}$ to estimate mutual information as per Eq .(2).
8: */* Sample Reweighting Module */*
9: Process sample loss l_O with the weighting net to produce dual weights as per Eq. (3), (4).
10: Adopt bi-level optimization to update the weighting net following Eq. (6), (7).
11: Re-calculate dual weights using the updated weighting net per Eq. (3), (4).
12: Calculate the overall loss to update the TS model as per Eq. (5).
13: **end while**
14: Return the trained TS model parameterized by $\boldsymbol{\theta}^*$.

LLM, where l denotes the language model. In this study, we employ the LLaMA-3b model (Touvron et al., 2023) as our primary LLM, while also evaluating other LLMs as detailed in Section 4.6.

We estimate mutual information using the Jensen-Shannon MI estimator (Sun et al., 2020; Nowozin et al., 2016) and additionally explore the MINE estimator (Hjelm et al., 2019a) as detailed in Appendix A.12. Specifically, let $(\boldsymbol{x}, \boldsymbol{t})$ represent a sample from the TS set $\mathbb{S}$, and $(\tilde{\boldsymbol{x}}, \tilde{\boldsymbol{t}})$ denote a sample from $\tilde{\mathbb{S}} = \mathbb{S}$ where $(\boldsymbol{x}, \boldsymbol{t}) \neq (\tilde{\boldsymbol{x}}, \tilde{\boldsymbol{t}})$. Within this context, $\mathbb{S}$ denotes the TS training distribution while the product $\mathbb{S} \times \tilde{\mathbb{S}}$ represents pairs of distinct samples within $\mathbb{S}$. Then the lower bound of mutual information can be estimated as:

$$I(\boldsymbol{\theta}, \boldsymbol{\beta}) = \mathbb{E}_{\mathbb{S}}[-sp(-T_{\boldsymbol{\beta}}(\boldsymbol{h}^m_{\boldsymbol{\theta}}(\boldsymbol{x}), \boldsymbol{h}^l(\boldsymbol{t}))] - \mathbb{E}_{\mathbb{S}\times\tilde{\mathbb{S}}}[sp(T_{\boldsymbol{\beta}}(\boldsymbol{h}^m_{\boldsymbol{\theta}}(\boldsymbol{x}), \boldsymbol{h}^l(\tilde{\boldsymbol{t}}))]\,, \tag{1}$$

where $T_{\boldsymbol{\beta}}$ denotes the discriminator parameterized by $\boldsymbol{\beta}$ and sp is the softplus function. For the details of T_{β}, we feed the positive and negative examples into a 1-layered fully-connected network with a hidden size of 64, and then output the dotproduct of the two representations. The mutual information estimation begins by fixing the model parameters $\boldsymbol{\theta}$, followed by training $\boldsymbol{\beta}$ as the estimator. Specifically, we optimize $\boldsymbol{\beta}$ via the following:

$$\hat{\boldsymbol{\beta}} = \boldsymbol{\beta} - \eta_0 \cdot \frac{\partial I(\boldsymbol{\theta}, \boldsymbol{\beta})}{\partial \boldsymbol{\beta}} \tag{2}$$

where η_0 denotes the learning rate. Subsequently, we refine the model parameters $\boldsymbol{\theta}$ to maximize mutual information, thereby enriching the traditional TS model with insights derived from LLMs. This alternating optimization procedure between model and discriminator is repeated each epoch.

3.1.2 Text Description for Time Series.

In our approach, we assume each time series (TS) sample $\boldsymbol{x}$ is paired with a corresponding textual description, $\boldsymbol{t}$. However, textual descriptions are frequently unavailable for many TS datasets. To bridge this gap, we introduce a methodology for generating textual descriptions of TS data. We propose creating textual representations that capture essential background and statistical details of the TS inspired by Jin et al. (2023). This process can be systematically implemented using the following carefully designed template:

```
template = (
    "{task_description}. The content is: {TS}. "
    "Input statistics: min value {min(TS)}, max value {max(TS)}, "
    "median value {median(TS)}, top 5 lags {compute_lags(TS)}."
)
```

3.2 Sample Reweighting

Our *mutual information* module introduces two distinct loss functions: (1) the original sample prediction loss, $l_O(\boldsymbol{x}, \boldsymbol{y})$, hereafter referred to as l_O, which corresponds to the prediction loss for a TS sample $\boldsymbol{x}$ and its label $\boldsymbol{y}$, and (2) the mutual information maximization loss, denoted as $-I(\boldsymbol{\theta}, \boldsymbol{\beta})$. We acknowledge that the significance of samples varies between these two losses. Specifically, a large prediction loss l_O indicates a sample's substantial learning potential, thereby justifying a higher weight ω_O for its prediction loss. Conversely, this suggests that the sample's representation may be suboptimal for mutual information computation, warranting a lower weight ω_I.

Here, $l_O(\boldsymbol{x}, \boldsymbol{y})$ denotes the sample-level loss for each task: For the forecasting task, we use MSE, where $\boldsymbol{y}$ represents the future target values. For the classification task, we use cross-entropy, where $\boldsymbol{y}$ corresponds to a class label. For the imputation task, we compute MSE for the masked points that need to be reconstructed. For the anomaly detection task, we adopt a reconstruction-based approach, measuring MSE between the original and reconstructed time series.

To address this disparity, we have developed a novel *sample reweighting* module, described as follows.

3.2.1 Weighting Network.

To automate weight assignment, our module employs a two-layer MLP network parameterized by $\boldsymbol{\alpha}$, which processes the sample prediction loss to produce a pair of weights:

$$\omega_O(\boldsymbol{\alpha}), \omega_I(\boldsymbol{\alpha}) = MLP_{\boldsymbol{\alpha}}(l_O) \tag{3}$$

This process involves converting the sample loss l_O into a latent code z through a hidden layer. The network then outputs dual weights:

$$\omega_O(\boldsymbol{\alpha}), \omega_I(\boldsymbol{\alpha}) = \sigma(m_O \cdot z), \sigma(m_I \cdot z) \tag{4}$$

where $m_O > 0$ and $m_I < 0$ to ensure a negative correlation between ω_O and ω_I. The function $\sigma(\cdot)$ denotes the sigmoid activation.

For a batch of N samples, the weight vector $\boldsymbol{\omega_O(\alpha)} \in \mathbb{R}^N$ is directly applied to the original prediction loss vector $\boldsymbol{l_O} \in \mathbb{R}^N$, resulting in the weighted average loss calculated as $mean(\boldsymbol{\omega_O}(\boldsymbol{\alpha}) \cdot \boldsymbol{l_O})$. Similarly, the weight vector $\boldsymbol{\omega_I(\alpha)} \in \mathbb{R}^N$ not only reflects the overall significance of the mutual information but also each sample's individual contribution to this metric. The mean of these weights $mean(\boldsymbol{\omega_I}(\boldsymbol{\alpha}))$ represents the overall importance. For mutual information computations, $\boldsymbol{\omega_I(\alpha)}$ is transformed into a probability distribution $p_I^i = \frac{\omega_I^i}{\sum_{i=1}^N \omega_I^i}$. This adjustment affects the distribution used in mutual information calculations, necessitating a recalculation of mutual information as $I(\boldsymbol{\theta}, \boldsymbol{\beta}, \boldsymbol{\alpha})$, with details provided in Appendix A.1. As a result, the overall loss is formulated as:

$$\mathcal{L}(\boldsymbol{\theta}, \boldsymbol{\alpha}) = mean(\boldsymbol{\omega_O}(\boldsymbol{\alpha}) \cdot \boldsymbol{l_O}) + mean(\boldsymbol{\omega_I}(\boldsymbol{\alpha})) \cdot [-I(\boldsymbol{\theta}, \boldsymbol{\beta}, \boldsymbol{\omega_I}(\boldsymbol{\alpha}))] \tag{5}$$

3.2.2 Bi-level Optimization.

The ensuing challenge is optimizing the weighting network $\boldsymbol{\alpha}$. We achieve this by leveraging the supervision signals from a small validation dataset (Chen et al., 2022). If the weighting network is properly optimized, the model trained with these weights is expected to show improved performance on the validation dataset in terms of the validation loss $\mathcal{L}_V(\boldsymbol{\theta}) = \frac{1}{M}\sum_j^M l_O^j(\boldsymbol{x}_j, \boldsymbol{y}_j)$, where M denotes the size of the validation set. This constitutes a bi-level optimization problem. At the inner level, model training is conducted through gradient descent:

$$\hat{\boldsymbol{\theta}}(\boldsymbol{\alpha}) = \boldsymbol{\theta} - \eta_1 \cdot \frac{\partial \mathcal{L}(\boldsymbol{\theta}, \boldsymbol{\alpha})}{\partial \boldsymbol{\theta}} \tag{6}$$

The objective is to ensure that the model performs optimally on the validation dataset:

$$\hat{\boldsymbol{\alpha}} = \boldsymbol{\alpha} - \eta_2 \cdot \frac{\partial \mathcal{L}_V(\boldsymbol{\theta}(\boldsymbol{\alpha}))}{\partial \boldsymbol{\alpha}} \tag{7}$$

Both η_1 and η_2 represent the learning rates for the respective optimization steps. Through the minimization of the validation loss, we aim to optimize the weighting network $\boldsymbol{\alpha}$.

4 Experimental Results

To demonstrate the versatility of our *LLM-TS Integrator*, we conduct extensive experiments across five main tasks: short- and long-term forecasting, imputation, classification, and anomaly detection. To maintain experimental integrity, our methodology adheres to the setup in (Wu et al., 2023). We detail the experimental setting in Appendix A.2.

4.0.1 Baselines.

Our evaluation employs a comprehensive array of baseline models across several architectural designs **(1)** CNN-based models, specifically TimesNet (Wu et al., 2023); **(2)** MLP-based models, including LightTS (Zhang et al., 2022) and DLinear (Zeng et al., 2023); **(3)** Transformer-based models, such as Reformer (Kitaev et al., 2020), Informer (Zhou et al., 2021b), Autoformer (Wu et al., 2021), FEDformer (Zhou et al., 2022), Nonstationary Transformer (Liu et al., 2022b), ETSformer (Woo et al., 2022), and PatchTST (Nie et al., 2023); **(4)** LLM-based models, represented by GPT4TS (Zhou et al., 2023). While we assess a wide range of models, we focus our discussion on the top-performing ones as highlighted in Zhou et al. (2023).

Additional comparisons for forecasting tasks include LLM-based models like Time-LLM (Jin et al., 2023) and TEST (Sun et al., 2023). For short-term forecasting, models like N-HiTS (Challu et al., 2023) and N-BEATS (Oreshkin et al., 2020) are included. Anomaly detection tasks are assessed using Anomaly Transformer (Xu et al., 2022), and for classification, models such as XGBoost (Chen and Guestrin, 2016), Rocket (Dempster et al., 2020), LSTNet (Lai et al., 2018), LSSL (Gu et al., 2022), Pyraformer (Liu et al., 2022a), TCN (Franceschi et al., 2019), and Flowformer (Huang et al., 2022) are considered. This broad selection of baselines enables a rigorous comparison across various tasks, highlighting the capabilities of our method.

4.1 Main Results

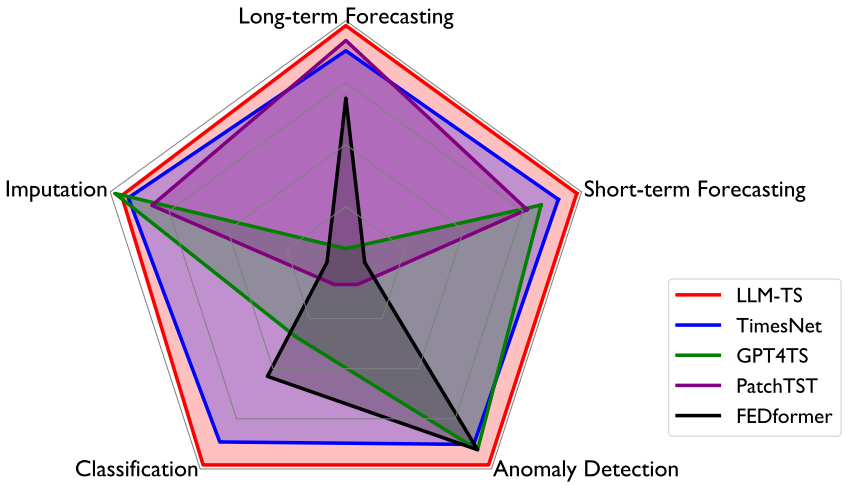

Figure 2: Model performance across different tasks.

Figure 2 demonstrates that our *LLM-TS Integrator* consistently outperforms other methods in various tasks, underscoring its efficacy. We will refer to our method as *LLM-TS* in the tables for brevity. Unless otherwise indicated, we cite results from TimesNet (Wu et al., 2023). We reproduce TimesNet and GPT4TS (Zhou et al., 2023) experiments for all tasks. All results are averages from three runs with different seeds. Standard deviations for ablation studies are detailed in Appendix 8. The best results are highlighted in bold, with the second-best underlined. We also (1) present several showcases of our method in Appendix A.4 and (2) discuss the model efficiency in Appendix A.6

4.2 Short- and Long- Term Forecasting

4.2.1 Setup.

To comprehensively assess our framework's forecasting capabilities, we engage it in both short- and long-term forecasting settings. In the realm of short-term forecasting, we utilize the M4 dataset (Spyros Makridakis, 2018), which aggregates univariate marketing data on a yearly, quarterly, and monthly basis. For long-term forecasting, we examine five datasets following (Zhou et al., 2023): ETT (Zhou et al., 2021a), Electricity (UCI, 2015), Traffic (PeMS, 2024), Weather (Wetterstation, 2024), and ILI (CDC, 2024). We adhere to the TimesNet setting with an input length of 96. For LLM-based methods like GPT4TS and Time-LLM, which use different input lengths, we rerun the experiments using their code. For PatchTST, we cite the results from (Wang et al., 2023a), as the original PatchTST uses an input length of 512. Due to shorter input lengths in this study compared to the original, the reported performance is lower.

4.2.2 Results.

As shown in Tables 1 and 2, our *LLM-TS* performs exceptionally well in both short- and long-term settings. It consistently surpasses TimesNet, highlighting the effectiveness of incorporating LLM-derived insights. Furthermore, it generally outperforms other LLM-based methods such as GPT4TS, TIME-LLM, and TEST, underscoring the advantages of integrating traditional TS modeling.

Table 1: Short-term M4 forecasting. The prediction lengths are in [6, 48] and results are obtained by weighting averages across multiple datasets with varying sampling intervals. Full results are in Appendix A.7.

Methods	LLM-TS	TimesNet	GPT4TS	TIME-LLM	TEST	PatchTST	N-HiTS	N-BEATS	FEDformer	Stationary	Autoformer
SMAPE	**11.819**	11.908	11.991	11.983	11.927	12.059	11.927	11.851	12.840	12.780	12.909
MASE	**1.588**	1.612	1.600	1.595	1.613	1.623	1.613	1.599	1.701	1.756	1.771
OWA	**0.851**	0.860	0.861	0.859	0.861	0.869	0.861	0.855	0.918	0.930	0.939

Table 2: Long-term forecasting: Averages over 4 lengths: 24, 36, 48, 60 for ILI, and 96, 192, 336, 720 for others. Full results in Appendix A.8.

Methods	LLM-TS		TimesNet		TIME-LLM		DLinear		PatchTST		GPT4TS		FEDformer		TEST		Stationary		ETSformer	
	MSE	MAE	MSE	MAE	MSE	MAE	MSE	MAE	MSE	MAE	MSE	MAE	MSE	MAE	MSE	MAE	MAE	MSE	MAE	MSE
Weather	**0.257**	**0.285**	0.265	0.290	0.279	0.296	0.265	0.317	0.265	**0.285**	0.275	0.292	0.309	0.360	0.291	0.315	0.288	0.314	0.271	0.334
ETTh1	0.454	**0.451**	0.470	0.462	0.474	0.459	0.456	0.452	0.516	0.484	0.473	**0.451**	**0.440**	0.460	**0.440**	0.460	0.570	0.537	0.542	0.510
ETTh2	0.396	0.413	0.413	0.426	0.398	0.415	0.559	0.515	0.391	**0.411**	**0.383**	0.410	0.437	0.449	0.414	0.432	0.526	0.516	0.439	0.452
ETTm1	**0.401**	0.409	0.414	0.418	0.437	0.421	0.403	0.407	0.406	0.407	0.408	**0.400**	0.448	0.452	0.402	0.411	0.481	0.456	0.429	0.425
ETTm2	0.295	**0.331**	0.294	**0.331**	0.298	0.342	0.350	0.401	**0.290**	0.334	**0.290**	0.335	0.305	0.349	0.323	0.359	0.306	0.347	0.293	0.342
ILI	**1.973**	**0.894**	2.266	0.974	2.726	1.098	2.616	1.090	2.184	0.906	5.117	1.650	2.847	1.144	3.324	1.232	2.077	0.914	2.497	1.004
ECL	0.194	0.299	0.198	0.298	0.229	0.315	0.212	0.300	0.216	0.318	0.206	**0.285**	0.214	0.327	0.237	0.324	**0.193**	0.296	0.208	0.323
Traffic	0.618	**0.333**	0.627	0.335	0.606	0.395	0.625	0.383	**0.529**	0.341	0.561	0.373	0.610	0.376	0.581	0.388	0.624	0.340	0.621	0.396
Average	**0.574**	**0.427**	0.618	0.442	0.681	0.468	0.686	0.483	0.600	0.436	0.964	0.525	0.701	0.489	0.756	0.491	0.633	0.465	0.662	0.473

4.3 Imputation

4.3.1 Setup.

To assess our method's imputation capabilities, we employ three datasets: ETT (Zhou et al., 2021a), Electricity (UCI, 2015), and Weather (Wetterstation, 2024), serving as our benchmarks. To simulate various degrees of missing data, we randomly obscure time points at proportions of $\{12.5\%, 25\%, 37.5\%, 50\%\}$ following (Wu et al., 2023).

4.3.2 Results.

Table 3 illustrates that our method achieves performance comparable to GPT4TS and surpasses other baselines, highlighting its effectiveness. We attribute the robust performance of GPT4TS primarily to its

backbone feature extractor: the pre-trained language model, which excels at capturing time series patterns, enhancing its imputation proficiency.

Table 3: Imputation task: Randomly masked {12.5%, 25%, 37.5%, 50%} of points in 96-length series, averaging results over 4 mask ratios. Full results are in Appendix A.9.

Methods	LLM-TS		TimesNet		GPT4TS		PatchTST		LightTS		DLinear		FEDformer		Stationary		Autoformer		Reformer	
	MSE	MAE	MSE	MAE	MSE	MAE	MSE	MAE	MSE	MAE	MSE	MAE	MSE	MAE	MSE	MAE	MSE	MAE	MSE	MAE
ETTm1	**0.025**	**0.103**	0.028	0.109	0.028	0.108	0.047	0.140	0.104	0.218	0.093	0.206	0.062	0.177	0.036	0.126	0.051	0.150	0.055	0.166
ETTm2	**0.021**	**0.087**	0.022	0.089	0.023	0.088	0.029	0.102	0.046	0.151	0.096	0.208	0.101	0.215	0.026	0.099	0.029	0.105	0.157	0.280
ETTh1	0.087	0.198	0.090	0.199	**0.069**	**0.174**	0.115	0.224	0.284	0.373	0.201	0.306	0.117	0.246	0.094	0.201	0.103	0.214	0.122	0.245
ETTh2	**0.050**	0.148	0.051	0.150	**0.050**	**0.144**	0.065	0.163	0.119	0.250	0.142	0.259	0.163	0.279	0.053	0.152	0.055	0.156	0.234	0.352
ECL	0.094	0.211	0.095	0.212	0.091	0.207	**0.072**	**0.183**	0.131	0.262	0.132	0.260	0.130	0.259	0.100	0.218	0.101	0.225	0.200	0.313
Weather	**0.030**	0.056	0.031	0.059	0.032	0.058	0.034	**0.055**	0.055	0.117	0.052	0.110	0.099	0.203	0.032	0.059	0.031	0.057	0.038	0.087
Average	0.051	0.134	0.053	0.136	**0.049**	**0.130**	0.060	0.144	0.123	0.228	0.119	0.224	0.112	0.229	0.056	0.142	0.061	0.151	0.134	0.240

4.4 Classification

4.4.1 Setup.

We focus on the application of our method to sequence-level time series classification tasks, a crucial test of its ability to learn high-level representations from data. Specifically, we employ 10 diverse multivariate datasets sourced from the UEA Time Series Classification repository (Bagnall et al., 2018). These datasets encompass a wide range of real-world applications, including gesture and action recognition, audio processing, among other practical domains. We reproduce the results of TEST based on their code (Sun et al., 2023).

4.4.2 Results.

As depicted in Figure 3, our *LLM-TS Integrator* achieves superior performance with an average accuracy of 73.4%. As detailed in Appendix A.10, it consistently outperforms other LLM-based methods across most tasks, including GPT4TS and TEST. We attribute this enhanced capability to the traditional TS modeling techniques in our framework, which effectively capture classification characteristics more adeptly than LLMs.

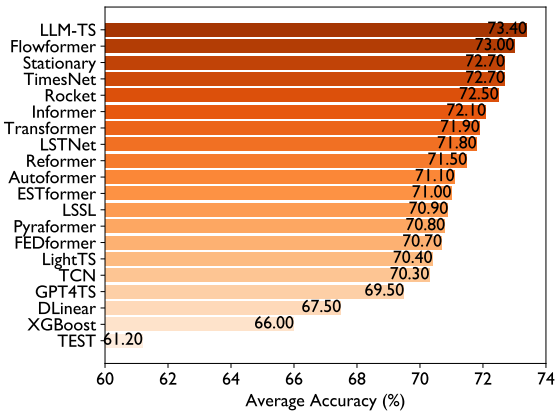

Figure 3: Model comparison in classification.

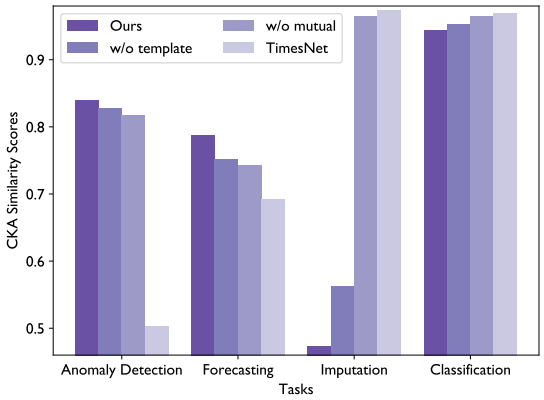

Figure 4: CKA by Task.

4.5 Anomaly Detection

4.5.1 Setup.

Our study concentrates on unsupervised time series anomaly detection, aiming to identify aberrant time points indicative of potential issues. We benchmark our method against five established anomaly detection

datasets: SMD (Su et al., 2019), MSL (Hundman et al., 2018), SMAP (Hundman et al., 2018), SWaT (Mathur and Tippenhauer, 2016), and PSM (Abdulaal et al., 2021). These datasets span a variety of applications, including service monitoring, space and earth exploration, and water treatment processes. For a consistent evaluation framework across all experiments, we employ the classical reconstruction error metric to determine anomalies following Wu et al. (2023).

4.5.2 Results.

As indicated in Table 4, our *LLM-TS Integrator* exhibits superior performance with an average F1-score of 85.17%. This result underscores the versatility of *LLM-TS*, demonstrating its capability not only in classifying complete sequences, as discussed previously, but also in effectively detecting anomalies in time series data.

Table 4: Anomaly detection task. F1-score (as %). $*$. in the Transformers represents the name of $*$former. Full results are in Appendix A.11.

Methods	LLM-TS	TimesNet	GPT4TS	PatchTS.	ETS.	FED.	LightTS	DLinear	Stationary	Auto.	Pyra.	Anomaly.**	In.	Re.	Trans.
SMD	84.69	84.57	84.32	84.62	83.13	85.08	82.53	77.10	84.72	85.11	83.04	85.49	81.65	75.32	79.56
MSL	81.11	80.34	81.73	78.70	85.03	78.57	78.95	84.88	77.50	79.05	84.86	83.31	84.06	84.40	78.68
SMAP	69.41	69.18	68.86	68.82	69.50	70.76	69.21	69.26	71.09	71.12	71.09	71.18	69.92	70.40	69.70
SWaT	93.23	93.12	92.59	85.72	84.91	93.19	93.33	87.52	79.88	92.74	91.78	83.10	81.43	82.80	80.37
PSM	97.43	97.27	97.34	96.08	91.76	97.23	97.15	93.55	97.29	93.29	82.08	79.40	77.10	73.61	76.07
Average	**85.17**	84.90	<u>84.97</u>	82.79	82.87	84.97	84.23	82.46	82.08	84.26	82.57	80.50	78.83	77.31	76.88

4.6 Ablations

In this section, we first verify the effectiveness of our framework by sequentially removing key components: (1) *mutual information* module and (2) *sample reweighting* module. Additionally, for *mutual information*, we explore the impact of removing the template while retaining the raw time series data inputs to the LLM. We denote these variants as *w/o mutual*, *w/o reweight* and *w/o template*. Our experiments span long-term forecasting tasks including Weather, ETTh1, ETTm1 and ILI. As detailed in Table 5, the removal of any component leads to a decrease in performance, confirming the value of each design element. Additionally, we explore the use of the MINE estimator (Hjelm et al., 2019a) instead of the Jensen-Shannon MI estimator in our main paper, with further details provided in Appendix A.12. Lastly, we showcase various case studies to demonstrate the enhancements facilitated by our method in Appendix A.4 and explore template variations in Appendix A.5.

4.6.1 Mutual Information.

We further explore the *mutual information* module from a representation learning perspective, following the findings in Wu et al. (2023). They adopt a CKA (Centered Kernel Alignment) metric which measures similarity between representations obtained from the first and last layer of a model and they find that

Table 5: Results averaged over 4 prediction lengths.

Methods	Ours		w/o mutual		w/o template		w/o reweight		TimesNet	
Metric	MSE	MAE	MSE	MAE	MSE	MAE	MSE	MAE	MSE	MAE
Weather	**0.257**	**0.285**	0.264	0.290	0.263	0.288	0.264	0.291	0.265	0.290
ETTh1	**0.454**	**0.451**	0.467	0.460	0.465	0.460	0.464	0.463	0.470	0.462
ETTh2	**0.396**	**0.413**	0.411	0.423	0.404	0.418	0.408	0.419	0.413	0.426
ETTm1	**0.401**	**0.409**	0.411	0.417	0.406	0.415	0.403	0.411	0.414	0.418
ETTm2	0.295	0.331	0.300	0.335	0.298	0.332	**0.292**	**0.328**	0.294	0.331
ILI	**1.973**	**0.894**	2.221	0.942	2.173	0.950	2.173	0.947	2.266	0.974
ECL	**0.194**	0.299	0.199	0.302	0.196	0.301	0.199	0.299	0.198	**0.298**
Traffic	**0.618**	**0.333**	0.624	0.336	0.622	0.335	0.622	0.336	0.627	0.335

forecasting and anomaly detection benefits from high CKA similarity, contrasting with that imputation and classification tasks benefits from lower CKA similarity.

Experiments are conducted using the MSL dataset for the anomaly detection task, the Weather dataset for forecasting, the ETTh1 dataset for imputation, and the PEMS-SF dataset for classification. As depicted in Figure 4, the removal of components in our method results in decreased CKA similarity in anomaly detection and forecasting tasks, but an increase in imputation and classification tasks. This observation further substantiates the effectiveness of our components.

4.6.2 Sample Reweighting.

Regarding the *sample reweighting* module, we illustrate the behavior of the learned weighting network in Appendix A.12. The trend confirms our hypothesis: sample weight ω_O increases with the prediction loss l_O, and weight ω_I decreases as l_O increases. This pattern validates our *sample reweighting* module. Further discussion comparing this module to a fixed weight scheme are presented in Appendix A.12.

To verify the effectiveness of our method, we conduct ablation studies focusing on (1) traditional time series (TS) models and (2) language models.

4.6.3 Traditional Models.

Although we utilize TimesNet as our primary model, our framework is applicable to other traditional models. We explored additional traditional models including ETSformer (Woo et al., 2022), Stationary (Liu et al., 2022b), and FreTS (Yi et al., 2023). As shown in Table 6, integrating *LLM-TS* generally enhances performance across all traditional models, underscoring the benefits of our method.

4.6.4 Language Models.

In the main paper, the LLaMA-3b model (Touvron et al., 2023) is used to generate embeddings for the TS language description. We compare it with GPT2 (Radford et al., 2019) and BERT (Devlin et al., 2019) to assess different embeddings' performance. Table 7 reveals that LLaMA-3b generally outperforms the alternatives, and all LMs improve results compared to non-LLM approaches, validating the effectiveness of *LLM-TS Integrator*.

Table 6: Ablation results on different traditional models. Full results are in Appendix A.12.

Methods	ETSformer		ETS LLM-TS		Stationary		Stat LLM-TS		FreTS		FreTS LLM-TS	
Metric	MSE	MAE	MSE	MAE	MSE	MAE	MSE	MAE	MSE	MAE	MSE	MAE
Weather	0.313	0.382	0.307	0.375	0.282	0.307	0.284	0.309	0.262	0.306	0.255	0.302
ETTh1	0.799	0.684	0.791	0.678	0.667	0.582	0.653	0.572	0.484	0.473	0.478	0.466
ETTm1	0.638	0.583	0.555	0.528	0.527	0.477	0.522	0.471	0.415	0.422	0.407	0.415
ILI	3.922	1.367	3.740	1.320	2.722	1.041	2.205	0.935	3.449	1.279	3.158	1.211

Table 7: Ablation results on different LLM embeddings. Full results are in Appendix A.12.

Methods	LLM-TS (LLaMA)		LLaMA w/o template		GPT2		BERT		No LLM	
Metric	MSE	MAE	MSE	MAE	MSE	MAE	MSE	MAE	MSE	MAE
Weather	**0.257**	**0.285**	0.263	0.288	0.261	0.287	0.260	0.287	0.264	0.290
ETTh1	**0.454**	**0.451**	0.465	0.460	0.464	0.458	0.467	0.460	0.467	0.460
ETTm1	**0.401**	**0.409**	0.406	0.415	0.406	0.413	0.406	0.412	0.411	0.417
ILI	**1.973**	**0.894**	2.173	0.950	2.169	0.936	2.193	0.952	2.221	0.942

5 Related Work

5.1 LLM for TS Modeling.

FPT (Zhou et al., 2023) suggests utilizing pre-trained language models to extract features from time series for improved predictions. TIME-LLM (Jin et al., 2024) and TEST (Sun et al., 2023) adapt LLMs for general time series forecasting by maintaining the original language model structure while reprogramming the input to fit time series data (Zhou et al., 2024). LLMTIME (Gruver et al., 2023b) interprets time series as sequences of numbers, treating forecasting as a next-token prediction task akin to text processing, applying pre-trained LLMs for this purpose. Given that it is not a state-of-the-art method and primarily targets zero-shot forecasting, it has not been incorporated into our experimental framework. TEMPO (Cao et al., 2024) utilizes essential inductive biases of the TS task for generative pre-trained transformer models. Gao et al. (2024); Goswami et al. (2024) also explore time series foundation models by pre-training large models on extensive time series datasets.

5.2 Time Series to Text.

PromptCast (Xue and Salim, 2023) proposes to transform the numerical input and output into prompts, which enables forecasting in a sentence-to-sentence manner. Time-LLM (Jin et al., 2024) incorporates background, instruction and statistical information of the time series data via natural language to facilitate time series forecasting in LLM. LLMTIME (Gruver et al., 2023a) converts time series data into a string of numbers and predicts future values as if completing a text. AutoTimes (Liu et al., 2024) maps time series into the embedding space of language tokens, enabling autoregressive generation of future predictions.

5.3 Mutual Information

The Infomax principle (Linsker, 1988; Bell and Sejnowski, 1995), applied in the context of neural networks, advocates for maximizing mutual information between the inputs and outputs of a network. Traditionally, quantifying mutual information was challenging outside a few specific probability distributions, as discussed in Shwartz-Ziv and Tishby (2017). This complexity led to the development of various heuristics and approximations (Tishby et al., 2000). Recently, a breakthrough came with MINE (Belghazi et al., 2021), which introduced a neural estimator capable of assessing mutual information between two arbitrary quantities with a precision that depends on the capacity of the encoding network. This innovative approach has spearheaded advancements in the field of representation learning (Hjelm et al., 2019b; Sylvain et al., 2020). The estimator we utilize is based on the Jensen-Shannon divergence variant of the MINE mutual information estimator.

5.4 Sample Reweighting.

Sample reweighting is commonly used to improve training efficacy (Fang et al., 2023; Wang et al., 2023b; Yuan et al., 2023a; Zhang et al., 2023; Yuan et al., 2023b). Traditional approaches (Freund and Schapire, 1997; Sun et al., 2007) assign larger weights to samples with higher loss values, as these hard samples have greater learning potential. Recent studies (Ren et al., 2018) suggest using a validation set to guide the learning of sample weights, which can enhance model training. Notably, meta-weight-net (Shu et al., 2019) proposes learning a mapping from sample loss to sample weight. In this work, we adopt an MLP network that takes sample prediction loss as input and outputs dual weights for prediction loss and mutual information loss.

6 Conclusion and Discussion

In conclusion, the *LLM-TS Integrator framework* offers a promising approach to integrating Large Language Models (LLMs) with traditional TS methods. By encouraging high mutual information between textual and TS data, our method aims to maintain the distinct characteristics of TS while benefiting from the advanced pattern recognition capabilities of LLMs. The introduced sample reweighting module enhances performance by dynamically adjusting the relevance of each sample based on its predictive and informational

contributions. Comprehensive empirical evaluations suggest that this framework improves accuracy across various TS tasks, including forecasting, anomaly detection, and classification. However, further research is necessary to confirm these results across more diverse and robust datasets including Monash (Godahewa et al., 2021) and GIFT-Eval (Aksu et al., 2024), and to explore additional LLM features that could further enrich our model. Additionally, it is important to acknowledge current limitations, such as the need for computational resources and the potential challenges in aligning the two modalities effectively.

References

Ahmed Abdulaal, Zhuanghua Liu, and Tomer Lancewicki. Practical approach to asynchronous multivariate time series anomaly detection and localization. In Feida Zhu, Beng Chin Ooi, and Chunyan Miao, editors, KDD '21: The 27th ACM SIGKDD Conference on Knowledge Discovery and Data Mining, Virtual Event, Singapore, August 14-18, 2021, pages 2485–2494. ACM, 2021. doi: 10.1145/3447548.3467174. URL https://doi.org/10.1145/3447548.3467174.

Taha Aksu, Gerald Woo, Juncheng Liu, Xu Liu, Chenghao Liu, Silvio Savarese, Caiming Xiong, and Doyen Sahoo. GIFT-eval: A benchmark for general time series forecasting model evaluation. In NeurIPS Workshop on Time Series in the Age of Large Models, 2024. URL https://openreview.net/forum?id=Z2cMOOANFX.

Anthony Bagnall, Hoang Anh Dau, Jason Lines, Michael Flynn, James Large, Aaron Bostrom, Paul Southam, and Eamonn Keogh. The uea multivariate time series classification archive, 2018. ArXiv preprint, abs/1811.00075, 2018. URL https://arxiv.org/abs/1811.00075.

Mohamed Ishmael Belghazi, Aristide Baratin, Sai Rajeswar, Sherjil Ozair, Yoshua Bengio, Aaron Courville, and R Devon Hjelm. Mine: Mutual information neural estimation, 2021.

Anthony J Bell and Terrence J Sejnowski. An information-maximization approach to blind separation and blind deconvolution. Neural computation, 7(6):1129–1159, 1995.

Tom B. Brown, Benjamin Mann, Nick Ryder, Melanie Subbiah, Jared Kaplan, Prafulla Dhariwal, Arvind Neelakantan, Pranav Shyam, Girish Sastry, Amanda Askell, Sandhini Agarwal, Ariel Herbert-Voss, Gretchen Krueger, Tom Henighan, Rewon Child, Aditya Ramesh, Daniel M. Ziegler, Jeffrey Wu, Clemens Winter, Christopher Hesse, Mark Chen, Eric Sigler, Mateusz Litwin, Scott Gray, Benjamin Chess, Jack Clark, Christopher Berner, Sam McCandlish, Alec Radford, Ilya Sutskever, and Dario Amodei. Language models are few-shot learners. In Hugo Larochelle, Marc'Aurelio Ranzato, Raia Hadsell, Maria-Florina Balcan, and Hsuan-Tien Lin, editors, Advances in Neural Information Processing Systems 33: Annual Conference on Neural Information Processing Systems 2020, NeurIPS 2020, December 6-12, 2020, virtual, 2020. URL https://proceedings.neurips.cc/paper/2020/hash/1457c0d6bfcb4967418bfb8ac142f64a-Abstract.html.

Defu Cao, Furong Jia, Sercan O Arik, Tomas Pfister, Yixiang Zheng, Wen Ye, and Yan Liu. Tempo: Prompt-based generative pre-trained transformer for time series forecasting. ICLR, 2024.

CDC. Illness. https://gis.cdc.gov/grasp/fluview/fluportaldashboard.html, 2024. Online; accessed 10 August 2024.

Cristian Challu, Kin G. Olivares, Boris N. Oreshkin, Federico Garza Ramírez, Max Mergenthaler Canseco, and Artur Dubrawski. NHITS: neural hierarchical interpolation for time series forecasting. In Brian Williams, Yiling Chen, and Jennifer Neville, editors, Thirty-Seventh AAAI Conference on Artificial Intelligence, AAAI 2023, Thirty-Fifth Conference on Innovative Applications of Artificial Intelligence, IAAI 2023, Thirteenth Symposium on Educational Advances in Artificial Intelligence, EAAI 2023, Washington, DC, USA, February 7-14, 2023, pages 6989–6997. AAAI Press, 2023. doi: 10.1609/AAAI.V37I6.25854. URL https://doi.org/10.1609/aaai.v37i6.25854.

Can Chen, Xi Chen, Chen Ma, Zixuan Liu, and Xue Liu. Gradient-based bi-level optimization for deep learning: A survey. ArXiv preprint, abs/2207.11719, 2022. URL https://arxiv.org/abs/2207.11719.

Tianqi Chen and Carlos Guestrin. Xgboost: A scalable tree boosting system. In Balaji Krishnapuram, Mohak Shah, Alexander J. Smola, Charu C. Aggarwal, Dou Shen, and Rajeev Rastogi, editors, Proceedings of the 22nd ACM SIGKDD International Conference on Knowledge Discovery and Data Mining, San Francisco, CA, USA, August 13-17, 2016, pages 785–794. ACM, 2016. doi: 10.1145/2939672.2939785. URL https://doi.org/10.1145/2939672.2939785.

Angus Dempster, François Petitjean, and Geoffrey I Webb. Rocket: exceptionally fast and accurate time series classification using random convolutional kernels. Data Mining and Knowledge Discovery, 34(5): 1454–1495, 2020.

Jacob Devlin, Ming-Wei Chang, Kenton Lee, and Kristina Toutanova. BERT: Pre-training of deep bidirectional transformers for language understanding. In Jill Burstein, Christy Doran, and Thamar Solorio, editors, Proceedings of the 2019 Conference of the North American Chapter of the Association for Computational Linguistics: Human Language Technologies, Volume 1 (Long and Short Papers), pages 4171–4186, Minneapolis, Minnesota, 2019. Association for Computational Linguistics. doi: 10.18653/v1/N19-1423. URL https://aclanthology.org/N19-1423.

Tongtong Fang, Nan Lu, Gang Niu, and Masashi Sugiyama. Generalizing importance weighting to A universal solver for distribution shift problems. In Alice Oh, Tristan Naumann, Amir Globerson, Kate Saenko, Moritz Hardt, and Sergey Levine, editors, Advances in Neural Information Processing Systems 36: Annual Conference on Neural Information Processing Systems 2023, NeurIPS 2023, New Orleans, LA, USA, December 10 - 16, 2023, 2023. URL http://papers.nips.cc/paper_files/paper/2023/hash/4c2092ec0b1370cce3fb5965ab255fae-Abstract-Conference.html.

Jean-Yves Franceschi, Aymeric Dieuleveut, and Martin Jaggi. Unsupervised scalable representation learning for multivariate time series. In Hanna M. Wallach, Hugo Larochelle, Alina Beygelzimer, Florence d'Alché-Buc, Emily B. Fox, and Roman Garnett, editors, Advances in Neural Information Processing Systems 32: Annual Conference on Neural Information Processing Systems 2019, NeurIPS 2019, December 8-14, 2019, Vancouver, BC, Canada, pages 4652–4663, 2019. URL https://proceedings.neurips.cc/paper/2019/hash/53c6de78244e9f528eb3e1cda69699bb-Abstract.html.

Luca Franceschi, Michele Donini, Paolo Frasconi, and Massimiliano Pontil. Forward and reverse gradient-based hyperparameter optimization. In Doina Precup and Yee Whye Teh, editors, Proceedings of the 34th International Conference on Machine Learning, ICML 2017, Sydney, NSW, Australia, 6-11 August 2017, volume 70 of Proceedings of Machine Learning Research, pages 1165–1173. PMLR, 2017. URL http://proceedings.mlr.press/v70/franceschi17a.html.

Yoav Freund and Robert E Schapire. A decision-theoretic generalization of on-line learning and an application to boosting. Journal of computer and system sciences, 1997.

Milton Friedman. The interpolation of time series by related series. Journal of the American Statistical Association, 1962.

Jingkun Gao, Xiaomin Song, Qingsong Wen, Pichao Wang, Liang Sun, and Huan Xu. Robusttad: Robust time series anomaly detection via decomposition and convolutional neural networks. ArXiv preprint, abs/2002.09545, 2020. URL https://arxiv.org/abs/2002.09545.

Shanghua Gao, Teddy Koker, Owen Queen, Tom Hartvigsen, Theodoros Tsiligkaridis, and Marinka Zitnik. Units: A unified multi-task time series model. Advances in Neural Information Processing Systems, 37: 140589–140631, 2024.

Rakshitha Godahewa, Christoph Bergmeir, Geoffrey I Webb, Rob J Hyndman, and Pablo Montero-Manso. Monash time series forecasting archive. ArXiv preprint, abs/2105.06643, 2021. URL https://arxiv.org/abs/2105.06643.

Mononito Goswami, Konrad Szafer, Arjun Choudhry, Yifu Cai, Shuo Li, and Artur Dubrawski. Moment: A family of open time-series foundation models. ArXiv preprint, abs/2402.03885, 2024. URL https://arxiv.org/abs/2402.03885.

Nate Gruver, Marc Finzi, Shikai Qiu, and Andrew Gordon Wilson. Large language models are zero-shot time series forecasters. In Alice Oh, Tristan Naumann, Amir Globerson, Kate Saenko, Moritz Hardt, and Sergey Levine, editors, Advances in Neural Information Processing Systems 36: Annual Conference on Neural Information Processing Systems 2023, NeurIPS 2023, New Orleans, LA, USA, December 10 - 16, 2023, 2023a. URL http://papers.nips.cc/paper_files/paper/2023/hash/3eb7ca52e8207697361b2c0fb3926511-Abstract-Conference.html.

Nate Gruver, Marc Finzi, Shikai Qiu, and Andrew Gordon Wilson. Large language models are zero-shot time series forecasters. In Alice Oh, Tristan Naumann, Amir Globerson, Kate Saenko, Moritz Hardt, and Sergey Levine, editors, Advances in Neural Information Processing Systems 36: Annual Conference on Neural Information Processing Systems 2023, NeurIPS 2023, New Orleans, LA, USA, December 10 - 16, 2023, 2023b. URL http://papers.nips.cc/paper_files/paper/2023/hash/3eb7ca52e8207697361b2c0fb3926511-Abstract-Conference.html.

Albert Gu, Karan Goel, and Christopher Ré. Efficiently modeling long sequences with structured state spaces. In The Tenth International Conference on Learning Representations, ICLR 2022, Virtual Event, April 25-29, 2022. OpenReview.net, 2022. URL https://openreview.net/forum?id=uYLFoz1vlAC.

R. Devon Hjelm, Alex Fedorov, Samuel Lavoie-Marchildon, Karan Grewal, Philip Bachman, Adam Trischler, and Yoshua Bengio. Learning deep representations by mutual information estimation and maximization. In 7th International Conference on Learning Representations, ICLR 2019, New Orleans, LA, USA, May 6-9, 2019. OpenReview.net, 2019a. URL https://openreview.net/forum?id=Bklr3j0cKX.

R. Devon Hjelm, Alex Fedorov, Samuel Lavoie-Marchildon, Karan Grewal, Philip Bachman, Adam Trischler, and Yoshua Bengio. Learning deep representations by mutual information estimation and maximization. In 7th International Conference on Learning Representations, ICLR 2019, New Orleans, LA, USA, May 6-9, 2019. OpenReview.net, 2019b. URL https://openreview.net/forum?id=Bklr3j0cKX.

Zhaoyang Huang, Xiaoyu Shi, Chao Zhang, Qiang Wang, Ka Chun Cheung, Hongwei Qin, Jifeng Dai, and Hongsheng Li. Flowformer: A transformer architecture for optical flow. In European conference on computer vision, pages 668–685. Springer, 2022.

Kyle Hundman, Valentino Constantinou, Christopher Laporte, Ian Colwell, and Tom Söderström. Detecting spacecraft anomalies using lstms and nonparametric dynamic thresholding. In Yike Guo and Faisal Farooq, editors, Proceedings of the 24th ACM SIGKDD International Conference on Knowledge Discovery & Data Mining, KDD 2018, London, UK, August 19-23, 2018, pages 387–395. ACM, 2018. doi: 10.1145/3219819.3219845. URL https://doi.org/10.1145/3219819.3219845.

Rob J Hyndman and George Athanasopoulos. Forecasting: principles and practice. OTexts, 2018.

Yushan Jiang, Zijie Pan, Xikun Zhang, Sahil Garg, Anderson Schneider, Yuriy Nevmyvaka, and Dongjin Song. Empowering time series analysis with large language models: A survey. ArXiv preprint, abs/2402.03182, 2024. URL https://arxiv.org/abs/2402.03182.

Ming Jin, Shiyu Wang, Lintao Ma, Zhixuan Chu, James Y Zhang, Xiaoming Shi, Pin-Yu Chen, Yuxuan Liang, Yuan-Fang Li, Shirui Pan, et al. Time-llm: Time series forecasting by reprogramming large language models. ArXiv preprint, abs/2310.01728, 2023. URL https://arxiv.org/abs/2310.01728.

Ming Jin, Shiyu Wang, Lintao Ma, Zhixuan Chu, James Y. Zhang, Xiaoming Shi, Pin-Yu Chen, Yuxuan Liang, Yuan-Fang Li, Shirui Pan, and Qingsong Wen. Time-LLM: Time series forecasting by reprogramming large language models. In The Twelfth International Conference on Learning Representations, 2024. URL https://openreview.net/forum?id=Unb5CVPtae.

Nikita Kitaev, Lukasz Kaiser, and Anselm Levskaya. Reformer: The efficient transformer. In 8th International Conference on Learning Representations, ICLR 2020, Addis Ababa, Ethiopia, April 26-30, 2020. OpenReview.net, 2020. URL https://openreview.net/forum?id=rkgNKkHtvB.

Guokun Lai, Wei-Cheng Chang, Yiming Yang, and Hanxiao Liu. Modeling long- and short-term temporal patterns with deep neural networks. In Kevyn Collins-Thompson, Qiaozhu Mei, Brian D. Davison, Yiqun Liu, and Emine Yilmaz, editors, The 41st International ACM SIGIR Conference on Research & Development in Information Retrieval, SIGIR 2018, Ann Arbor, MI, USA, July 08-12, 2018, pages 95–104. ACM, 2018. doi: 10.1145/3209978.3210006. URL https://doi.org/10.1145/3209978.3210006.

Bryan Lim and Stefan Zohren. Time-series forecasting with deep learning: a survey. Philos. Trans. Royal Soc. A, 2021.

Ralph Linsker. Self-organization in a perceptual network. Computer, 21:105–117, 1988. URL https://api.semanticscholar.org/CorpusID:1527671.

Shizhan Liu, Hang Yu, Cong Liao, Jianguo Li, Weiyao Lin, Alex X. Liu, and Schahram Dustdar. Pyraformer: Low-complexity pyramidal attention for long-range time series modeling and forecasting. In The Tenth International Conference on Learning Representations, ICLR 2022, Virtual Event, April 25-29, 2022. OpenReview.net, 2022a. URL https://openreview.net/forum?id=0EXmFzUn5I.

Yong Liu, Haixu Wu, Jianmin Wang, and Mingsheng Long. Non-stationary transformers: Exploring the stationarity in time series forecasting. In Sanmi Koyejo, S. Mohamed, A. Agarwal, Danielle Belgrave, K. Cho, and A. Oh, editors, Advances in Neural Information Processing Systems 35: Annual Conference on Neural Information Processing Systems 2022, NeurIPS 2022, New Orleans, LA, USA, November 28 - December 9, 2022, 2022b. URL http://papers.nips.cc/paper_files/paper/2022/hash/4054556fcaa934b0bf76da52cf4f92cb-Abstract-Conference.html.

Yong Liu, Guo Qin, Xiangdong Huang, Jianmin Wang, and Mingsheng Long. Autotimes: Autoregressive time series forecasters via large language models. ArXiv preprint, abs/2402.02370, 2024. URL https://arxiv.org/abs/2402.02370.

Aditya P. Mathur and Nils Ole Tippenhauer. Swat: a water treatment testbed for research and training on ICS security. In CySWATER, 2016.

Yuqi Nie, Nam H. Nguyen, Phanwadee Sinthong, and Jayant Kalagnanam. A time series is worth 64 words: Long-term forecasting with transformers. In The Eleventh International Conference on Learning Representations, ICLR 2023, Kigali, Rwanda, May 1-5, 2023. OpenReview.net, 2023. URL https://openreview.net/pdf?id=Jbdc0vTOcol.

Sebastian Nowozin, Botond Cseke, and Ryota Tomioka. f-gan: Training generative neural samplers using variational divergence minimization. In Daniel D. Lee, Masashi Sugiyama, Ulrike von Luxburg, Isabelle Guyon, and Roman Garnett, editors, Advances in Neural Information Processing Systems 29: Annual Conference on Neural Information Processing Systems 2016, December 5-10, 2016, Barcelona, Spain, pages 271–279, 2016. URL https://proceedings.neurips.cc/paper/2016/hash/cedebb6e872f539bef8c3f919874e9d7-Abstract.html.

Boris N. Oreshkin, Dmitri Carpov, Nicolas Chapados, and Yoshua Bengio. N-BEATS: neural basis expansion analysis for interpretable time series forecasting. In 8th International Conference on Learning Representations, ICLR 2020, Addis Ababa, Ethiopia, April 26-30, 2020. OpenReview.net, 2020. URL https://openreview.net/forum?id=r1ecqn4YwB.

PeMS. Traffic. http://pems.dot.ca.gov/, 2024. Online; accessed 10 August 2024.

Alec Radford, Jeffrey Wu, Rewon Child, David Luan, Dario Amodei, Ilya Sutskever, et al. Language models are unsupervised multitask learners. OpenAI blog, 2019.

Mengye Ren, Wenyuan Zeng, Bin Yang, and Raquel Urtasun. Learning to reweight examples for robust deep learning. In Jennifer G. Dy and Andreas Krause, editors, Proceedings of the 35th International Conference on Machine Learning, ICML 2018, Stockholmsmässan, Stockholm, Sweden, July 10-15, 2018, volume 80 of Proceedings of Machine Learning Research, pages 4331–4340. PMLR, 2018. URL http://proceedings.mlr.press/v80/ren18a.html.

Jun Shu, Qi Xie, Lixuan Yi, Qian Zhao, Sanping Zhou, Zongben Xu, and Deyu Meng. Meta-weight-net: Learning an explicit mapping for sample weighting. In Hanna M. Wallach, Hugo Larochelle, Alina Beygelzimer, Florence d'Alché-Buc, Emily B. Fox, and Roman Garnett, editors, Advances in Neural Information Processing Systems 32: Annual Conference on Neural Information Processing Systems 2019, NeurIPS 2019, December 8-14, 2019, Vancouver, BC, Canada, pages 1917–1928, 2019. URL https://proceedings.neurips.cc/paper/2019/hash/e58cc5ca94270acaceed13bc82dfedf7-Abstract.html.

Ravid Shwartz-Ziv and Naftali Tishby. Opening the black box of deep neural networks via information, 2017.

Spyros Makridakis. M4 dataset, 2018. URL https://github.com/M4Competition/M4-methods/tree/master/Dataset.

Ya Su, Youjian Zhao, Chenhao Niu, Rong Liu, Wei Sun, and Dan Pei. Robust anomaly detection for multivariate time series through stochastic recurrent neural network. In Ankur Teredesai, Vipin Kumar, Ying Li, Rómer Rosales, Evimaria Terzi, and George Karypis, editors, Proceedings of the 25th ACM SIGKDD International Conference on Knowledge Discovery & Data Mining, KDD 2019, Anchorage, AK, USA, August 4-8, 2019, pages 2828–2837. ACM, 2019. doi: 10.1145/3292500.3330672. URL https://doi.org/10.1145/3292500.3330672.

Chenxi Sun, Yaliang Li, Hongyan Li, and Shenda Hong. Test: Text prototype aligned embedding to activate llm's ability for time series. ArXiv preprint, abs/2308.08241, 2023. URL https://arxiv.org/abs/2308.08241.

Fan-Yun Sun, Jordan Hoffmann, Vikas Verma, and Jian Tang. Infograph: Unsupervised and semi-supervised graph-level representation learning via mutual information maximization. In 8th International Conference on Learning Representations, ICLR 2020, Addis Ababa, Ethiopia, April 26-30, 2020. OpenReview.net, 2020. URL https://openreview.net/forum?id=r1lfF2NYvH.

Yanmin Sun, Mohamed S Kamel, Andrew KC Wong, and Yang Wang. Cost-sensitive boosting for classification of imbalanced data. Pattern recognition, 2007.

Tristan Sylvain, Linda Petrini, and R. Devon Hjelm. Locality and compositionality in zero-shot learning. In 8th International Conference on Learning Representations, ICLR 2020, Addis Ababa, Ethiopia, April 26-30, 2020. OpenReview.net, 2020. URL https://openreview.net/forum?id=Hye_V0NKwr.

Mingtian Tan, Mike Merrill, Vinayak Gupta, Tim Althoff, and Tom Hartvigsen. Are language models actually useful for time series forecasting? Advances in Neural Information Processing Systems, 37:60162–60191, 2024.

Naftali Tishby, Fernando C. Pereira, and William Bialek. The information bottleneck method, 2000.

Hugo Touvron, Louis Martin, Kevin Stone, Peter Albert, Amjad Almahairi, Yasmine Babaei, Nikolay Bashlykov, Soumya Batra, Prajjwal Bhargava, Shruti Bhosale, et al. Llama 2: Open foundation and fine-tuned chat models. ArXiv preprint, abs/2307.09288, 2023. URL https://arxiv.org/abs/2307.09288.

UCI. Electricity. https://archive.ics.uci.edu/ml/datasets/ElectricityLoadDiagrams20112014, 2015. Online; accessed 10 August 2024.

Shiyu Wang, Haixu Wu, Xiaoming Shi, Tengge Hu, Huakun Luo, Lintao Ma, James Y Zhang, and JUN ZHOU. Timemixer: Decomposable multiscale mixing for time series forecasting. In ICLR, 2023a.

Zitai Wang, Qianqian Xu, Zhiyong Yang, Yuan He, Xiaochun Cao, and Qingming Huang. A unified generalization analysis of re-weighting and logit-adjustment for imbalanced learning. In Alice Oh, Tristan Naumann, Amir Globerson, Kate Saenko, Moritz Hardt, and Sergey Levine, editors, Advances in Neural Information Processing Systems 36: Annual Conference on Neural Information Processing Systems 2023, NeurIPS 2023, New Orleans, LA, USA, December 10 - 16, 2023, 2023b. URL http://papers.nips.cc/paper_files/paper/2023/hash/973a0f50d43cf99118cdab456edcacda-Abstract-Conference.html.

Qingsong Wen, Linxiao Yang, Tian Zhou, and Liang Sun. Robust time series analysis and applications: An industrial perspective. In Aidong Zhang and Huzefa Rangwala, editors, KDD '22: The 28th ACM SIGKDD Conference on Knowledge Discovery and Data Mining, Washington, DC, USA, August 14 - 18, 2022, pages 4836–4837. ACM, 2022. doi: 10.1145/3534678.3542612. URL https://doi.org/10.1145/3534678.3542612.

Wetterstation. Weather. https://www.bgc-jena.mpg.de/wetter/, 2024. Online; accessed 10 August 2024.

Gerald Woo, Chenghao Liu, Doyen Sahoo, Akshat Kumar, and Steven C. H. Hoi. Etsformer: Exponential smoothing transformers for time-series forecasting. ArXiv preprint, abs/2202.01381, 2022. URL https://arxiv.org/abs/2202.01381.

Haixu Wu, Jiehui Xu, Jianmin Wang, and Mingsheng Long. Autoformer: Decomposition transformers with auto-correlation for long-term series forecasting. In Marc'Aurelio Ranzato, Alina Beygelzimer, Yann N. Dauphin, Percy Liang, and Jennifer Wortman Vaughan, editors, Advances in Neural Information Processing Systems 34: Annual Conference on Neural Information Processing Systems 2021, NeurIPS 2021, December 6-14, 2021, virtual, pages 22419–22430, 2021. URL https://proceedings.neurips.cc/paper/2021/hash/bcc0d400288793e8bdcd7c19a8ac0c2b-Abstract.html.

Haixu Wu, Tengge Hu, Yong Liu, Hang Zhou, Jianmin Wang, and Mingsheng Long. Timesnet: Temporal 2d-variation modeling for general time series analysis. In The Eleventh International Conference on Learning Representations, ICLR 2023, Kigali, Rwanda, May 1-5, 2023. OpenReview.net, 2023. URL https://openreview.net/pdf?id=ju_Uqw384Oq.

Jiehui Xu, Haixu Wu, Jianmin Wang, and Mingsheng Long. Anomaly transformer: Time series anomaly detection with association discrepancy. In The Tenth International Conference on Learning Representations, ICLR 2022, Virtual Event, April 25-29, 2022. OpenReview.net, 2022. URL https://openreview.net/forum?id=LzQQ89U1qm_.

Hao Xue and Flora D Salim. Promptcast: A new prompt-based learning paradigm for time series forecasting. IEEE Transactions on Knowledge and Data Engineering, 2023.

Kun Yi, Qi Zhang, Wei Fan, Shoujin Wang, Pengyang Wang, Hui He, Ning An, Defu Lian, Longbing Cao, and Zhendong Niu. Frequency-domain mlps are more effective learners in time series forecasting. In Alice Oh, Tristan Naumann, Amir Globerson, Kate Saenko, Moritz Hardt, and Sergey Levine, editors, Advances in Neural Information Processing Systems 36: Annual Conference on Neural Information Processing Systems 2023, NeurIPS 2023, New Orleans, LA, USA, December 10 - 16, 2023, 2023. URL http://papers.nips.cc/paper_files/paper/2023/hash/f1d16af76939f476b5f040fd1398c0a3-Abstract-Conference.html.

Huining Yuan, Hongkun Dou, Xingyu Jiang, and Yue Deng. Task-aware world model learning with meta weighting via bi-level optimization. In Alice Oh, Tristan Naumann, Amir Globerson, Kate Saenko, Moritz Hardt, and Sergey Levine, editors, Advances in Neural Information Processing Systems 36: Annual Conference on Neural Information Processing Systems 2023, NeurIPS 2023, New Orleans, LA, USA, December 10 - 16, 2023, 2023a. URL http://papers.nips.cc/paper_files/paper/2023/hash/a995960dd0193654d6b18eca4ac5b936-Abstract-Conference.html.

Ye Yuan, Can Chen, Zixuan Liu, Willie Neiswanger, and Xue (Steve) Liu. Importance-aware co-teaching for offline model-based optimization. In Alice Oh, Tristan Naumann, Amir Globerson, Kate Saenko, Moritz Hardt, and Sergey Levine, editors, Advances in Neural Information Processing Systems 36: Annual Conference on Neural Information Processing Systems 2023, NeurIPS 2023, New Orleans, LA, USA, December 10 - 16, 2023, 2023b. URL http://papers.nips.cc/paper_files/paper/2023/hash/ae8b0b5838ba510daff1198474e7b984-Abstract-Conference.html.

Ailing Zeng, Muxi Chen, Lei Zhang, and Qiang Xu. Are transformers effective for time series forecasting? In Brian Williams, Yiling Chen, and Jennifer Neville, editors, Thirty-Seventh AAAI Conference on Artificial Intelligence, AAAI 2023, Thirty-Fifth Conference on Innovative Applications of Artificial Intelligence, IAAI 2023, Thirteenth Symposium on Educational Advances in Artificial Intelligence, EAAI 2023, Washington, DC, USA, February 7-14, 2023, pages 11121–11128. AAAI Press, 2023. doi: 10.1609/AAAI.V37I9.26317. URL https://doi.org/10.1609/aaai.v37i9.26317.

Tianping Zhang, Yizhuo Zhang, Wei Cao, Jiang Bian, Xiaohan Yi, Shun Zheng, and Jian Li. Less is more: Fast multivariate time series forecasting with light sampling-oriented mlp structures. ArXiv preprint, abs/2207.01186, 2022. URL https://arxiv.org/abs/2207.01186.

Xiaoying Zhang, Junpu Chen, Hongning Wang, Hong Xie, Yang Liu, John C. S. Lui, and Hang Li. Uncertainty-aware instance reweighting for off-policy learning. In Alice Oh, Tristan Naumann, Amir Globerson, Kate Saenko, Moritz Hardt, and Sergey Levine, editors, Advances in Neural Information Processing Systems 36: Annual Conference on Neural Information Processing Systems 2023, NeurIPS 2023, New Orleans, LA, USA, December 10 - 16, 2023, 2023. URL http://papers.nips.cc/paper_files/paper/2023/hash/e97ac22927560eb2de6b658498cbc575-Abstract-Conference.html.

Hao Zhou, Chengming Hu, Ye Yuan, Yufei Cui, Yili Jin, Can Chen, Haolun Wu, Dun Yuan, Li Jiang, Di Wu, et al. Large language model (llm) for telecommunications: A comprehensive survey on principles, key techniques, and opportunities. ArXiv preprint, abs/2405.10825, 2024. URL https://arxiv.org/abs/2405.10825.

Haoyi Zhou, Shanghang Zhang, Jieqi Peng, Shuai Zhang, Jianxin Li, Hui Xiong, and Wancai Zhang. Informer: Beyond efficient transformer for long sequence time-series forecasting. In Thirty-Fifth AAAI Conference on Artificial Intelligence, AAAI 2021, Thirty-Third Conference on Innovative Applications of Artificial Intelligence, IAAI 2021, The Eleventh Symposium on Educational Advances in Artificial Intelligence, EAAI 2021, Virtual Event, February 2-9, 2021, pages 11106–11115. AAAI Press, 2021a. URL https://ojs.aaai.org/index.php/AAAI/article/view/17325.

Haoyi Zhou, Shanghang Zhang, Jieqi Peng, Shuai Zhang, Jianxin Li, Hui Xiong, and Wancai Zhang. Informer: Beyond efficient transformer for long sequence time-series forecasting. In Thirty-Fifth AAAI Conference on Artificial Intelligence, AAAI 2021, Thirty-Third Conference on Innovative Applications of Artificial Intelligence, IAAI 2021, The Eleventh Symposium on Educational Advances in Artificial Intelligence, EAAI 2021, Virtual Event, February 2-9, 2021, pages 11106–11115. AAAI Press, 2021b. URL https://ojs.aaai.org/index.php/AAAI/article/view/17325.

Tian Zhou, Ziqing Ma, Qingsong Wen, Xue Wang, Liang Sun, and Rong Jin. Fedformer: Frequency enhanced decomposed transformer for long-term series forecasting. In Kamalika Chaudhuri, Stefanie Jegelka, Le Song, Csaba Szepesvári, Gang Niu, and Sivan Sabato, editors, International Conference on Machine Learning, ICML 2022, 17-23 July 2022, Baltimore, Maryland, USA, volume 162 of Proceedings of Machine Learning Research, pages 27268–27286. PMLR, 2022. URL https://proceedings.mlr.press/v162/zhou22g.html.

Tian Zhou, Peisong Niu, Xue Wang, Liang Sun, and Rong Jin. One fits all: Power general time series analysis by pretrained LM. In Alice Oh, Tristan Naumann, Amir Globerson, Kate Saenko, Moritz Hardt, and Sergey Levine, editors, Advances in Neural Information Processing Systems 36: Annual Conference on Neural Information Processing Systems 2023, NeurIPS 2023, New Orleans, LA, USA, December 10 - 16, 2023, 2023. URL http://papers.nips.cc/paper_files/paper/2023/hash/86c17de05579cde52025f9984e6e2ebb-Abstract-Conference.html.

A Appendix

A.1 Mutual Information Recalculation

Recall that mutual information can be calculated using the equation:

$$I(\boldsymbol{\theta}, \boldsymbol{\beta}) = \mathbb{E}_{\mathbb{S}}[-sp(-T_{\boldsymbol{\beta}}(\boldsymbol{h}_{\boldsymbol{\theta}}^{m}(\boldsymbol{x}), \boldsymbol{h}^{l}(\boldsymbol{t}))] - \mathbb{E}_{\mathbb{S}\times\tilde{\mathbb{S}}}[sp(T_{\boldsymbol{\beta}}(\boldsymbol{h}_{\boldsymbol{\theta}}^{m}(\boldsymbol{x}), \boldsymbol{h}^{l}(\tilde{\boldsymbol{t}}))]\,, \tag{8}$$

where $T_{\boldsymbol{\beta}}$ signifies the discriminator characterized by parameters $\boldsymbol{\beta}$, and sp denotes the softplus function. Notably, $(\boldsymbol{x}, \boldsymbol{t})$ symbolizes a sample from the dataset $\mathbb{S}$, while $(\tilde{\boldsymbol{x}}, \tilde{\boldsymbol{t}})$ represents a different sample from the dataset $\tilde{\mathbb{S}} = \mathbb{S}$.

This formulation presumes a uniform distribution of samples. However, we have already computed probabilities p_I^i for each sample, which introduces a non-uniform distribution. For a batch of N samples, the expected value is computed as

$$\mathbb{E}_{\mathbb{S}}[-sp(-T_{\boldsymbol{\beta}}(\boldsymbol{h}_{\boldsymbol{\theta}}^m(\boldsymbol{x}), \boldsymbol{h}^l(\boldsymbol{t}))] = -\sum_{i=1}^{N} p_I^i sp(-T_{\boldsymbol{\beta}}(\boldsymbol{h}_{\boldsymbol{\theta}}^m(\boldsymbol{x}^{\boldsymbol{i}}), \boldsymbol{h}^l(\boldsymbol{t}^{\boldsymbol{i}})). \tag{9}$$

$$\mathbb{E}_{\mathbb{S}\times\tilde{\mathbb{S}}}[sp(T_{\boldsymbol{\beta}}(\boldsymbol{h}_{\boldsymbol{\theta}}^m(\boldsymbol{x}), \boldsymbol{h}^l(\tilde{\boldsymbol{t}}))] = \sum_i \sum_{i\neq j} \hat{p}^{ij} sp(T_{\boldsymbol{\beta}}(\boldsymbol{h}_{\boldsymbol{\theta}}^m(\boldsymbol{x}^{\boldsymbol{i}}), \boldsymbol{h}^l(\tilde{\boldsymbol{t}}^{\boldsymbol{j}})). \tag{10}$$

Here, $\hat{p}^{ij}$ is defined as $\frac{p_I^i \cdot p_I^j}{\sum_i \sum_{i\neq j} p_I^i \cdot p_I^j}$, adjusting for the non-uniform distribution of sample probabilities. As p_I^i is produced from the weighting network $\boldsymbol{\alpha}$, we can also write $I(\boldsymbol{\theta}, \boldsymbol{\beta})$ as $I(\boldsymbol{\theta}, \boldsymbol{\beta}, \boldsymbol{\alpha})$.

A.2 Experimental Settings

Following Shu et al. (2019), the weighting network comprises a two-layer MLP with a hidden size of 100, and we set the learning rate η_2 for this network at 0.001. The learning rate η_0 of the discriminator is set as 0.001 at the first epoch and then decreases to 0.0001 for the rest of epochs.

A.3 Standard Error Results

Table 8 presents the results along with standard errors to underscore the consistency and reliability of our method's performance.

Table 8: Ablation results with standard error.

Methods		Ours		w/o mutual		w/o reweight		TimesNet	
Metric		MSE	MAE	MSE	MAE	MSE	MAE	MSE	MAE
Weather	96	0.166 ± 0.001	0.217 ± 0.001	0.168 ± 0.002	0.218 ± 0.003	0.181 ± 0.002	0.232 ± 0.001	0.174 ± 0.002	0.224 ± 0.001
	192	0.229 ± 0.002	0.269 ± 0.002	0.227 ± 0.002	0.268 ± 0.002	0.230 ± 0.001	0.270 ± 0.002	0.235 ± 0.001	0.272 ± 0.002
	336	0.278 ± 0.001	0.302 ± 0.002	0.298 ± 0.002	0.318 ± 0.002	0.283 ± 0.002	0.306 ± 0.001	0.285 ± 0.002	0.307 ± 0.001
	720	0.354 ± 0.001	0.351 ± 0.001	0.361 ± 0.001	0.356 ± 0.001	0.361 ± 0.001	0.355 ± 0.001	0.365 ± 0.001	0.358 ± 0.000
ETTh1	96	0.403 ± 0.003	0.420 ± 0.002	0.402 ± 0.002	0.422 ± 0.001	0.408 ± 0.002	0.428 ± 0.001	0.414 ± 0.003	0.431 ± 0.002
	192	0.440 ± 0.005	0.441 ± 0.002	0.459 ± 0.003	0.455 ± 0.003	0.469 ± 0.003	0.460 ± 0.002	0.463 ± 0.006	0.456 ± 0.003
	336	0.471 ± 0.003	0.457 ± 0.002	0.471 ± 0.003	0.457 ± 0.002	0.492 ± 0.002	0.474 ± 0.002	0.487 ± 0.004	0.466 ± 0.003
	720	0.503 ± 0.003	0.487 ± 0.002	0.535 ± 0.002	0.507 ± 0.002	0.485 ± 0.003	0.478 ± 0.004	0.517 ± 0.002	0.494 ± 0.002
ETTm1	96	0.329 ± 0.008	0.371 ± 0.004	0.341 ± 0.006	0.377 ± 0.005	0.350 ± 0.006	0.387 ± 0.003	0.340 ± 0.006	0.377 ± 0.004
	192	0.380 ± 0.005	0.398 ± 0.002	0.404 ± 0.006	0.413 ± 0.003	0.383 ± 0.006	0.397 ± 0.003	0.406 ± 0.007	0.408 ± 0.002
	336	0.418 ± 0.002	0.425 ± 0.002	0.432 ± 0.003	0.428 ± 0.001	0.410 ± 0.002	0.411 ± 0.002	0.424 ± 0.003	0.425 ± 0.002
	720	0.476 ± 0.005	0.440 ± 0.003	0.468 ± 0.005	0.449 ± 0.002	0.467 ± 0.004	0.448 ± 0.002	0.485 ± 0.006	0.461 ± 0.004
ILI	24	1.921 ± 0.116	0.898 ± 0.019	2.170 ± 0.100	0.947 ± 0.023	1.934 ± 0.098	0.925 ± 0.020	2.072 ± 0.122	0.948 ± 0.015
	36	2.151 ± 0.035	0.933 ± 0.020	2.093 ± 0.069	0.889 ± 0.024	2.505 ± 0.103	1.020 ± 0.010	2.494 ± 0.072	1.019 ± 0.004
	48	2.062 ± 0.052	0.892 ± 0.011	2.418 ± 0.034	0.959 ± 0.008	2.325 ± 0.116	0.948 ± 0.036	2.298 ± 0.038	0.964 ± 0.006
	60	1.759 ± 0.124	0.853 ± 0.035	2.203 ± 0.105	0.971 ± 0.028	1.926 ± 0.088	0.896 ± 0.023	2.198 ± 0.040	0.963 ± 0.010

A.4 Showcases

To provide a clear comparison among different models, we showcase the forecasting task results on ETTh1 (96-96) and ETTm1 (96-336) using three models: *LLM-TS*, TimesNet, and GPT4TS. As shown in Figures 5 and 6, our LLM-TS model produces significantly more accurate predictions, demonstrating its effectiveness.

To illustrate the performance improvements achieved by the LLM-TS Integrator framework, we introduce a case study. We created a training set with a weighted sine function:

$$\sum_{i=1}^{4} \omega_i \sin(f_i t + p_i) + \epsilon N(0, 1) \tag{11}$$

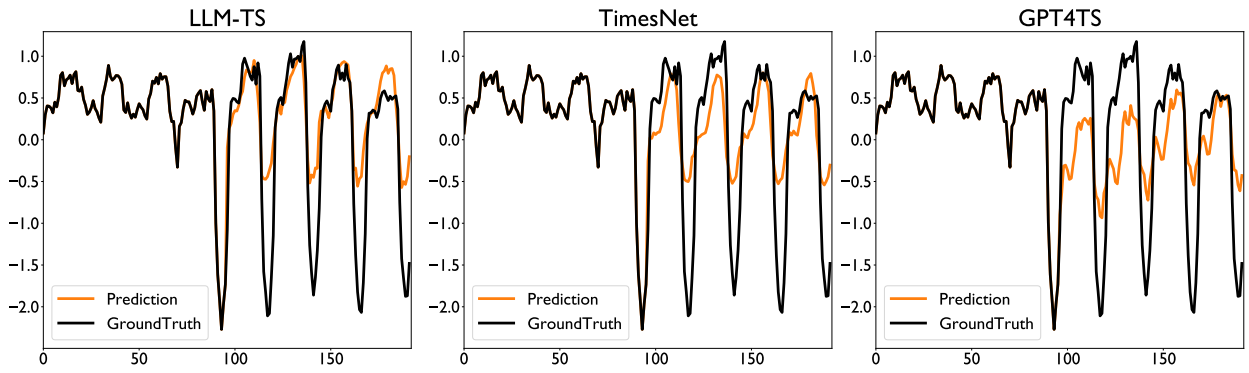

Figure 5: ETTh1

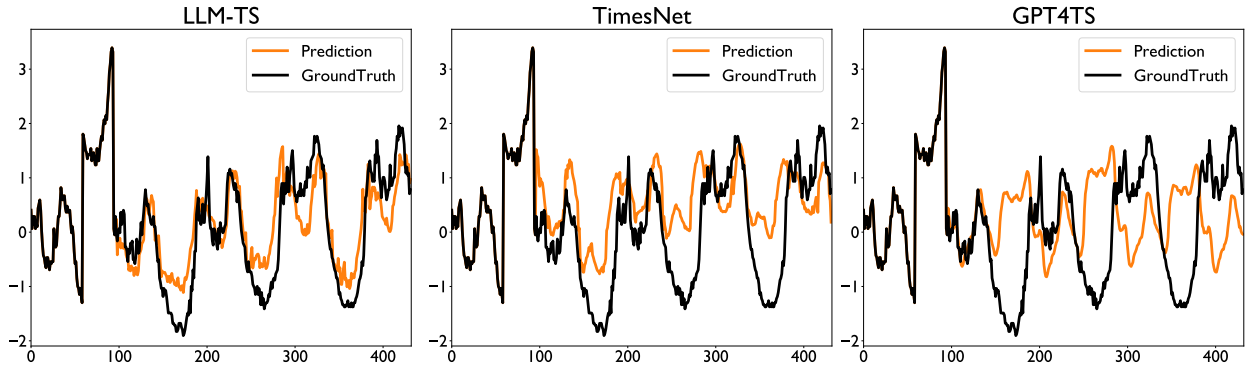

Figure 6: ETTm1

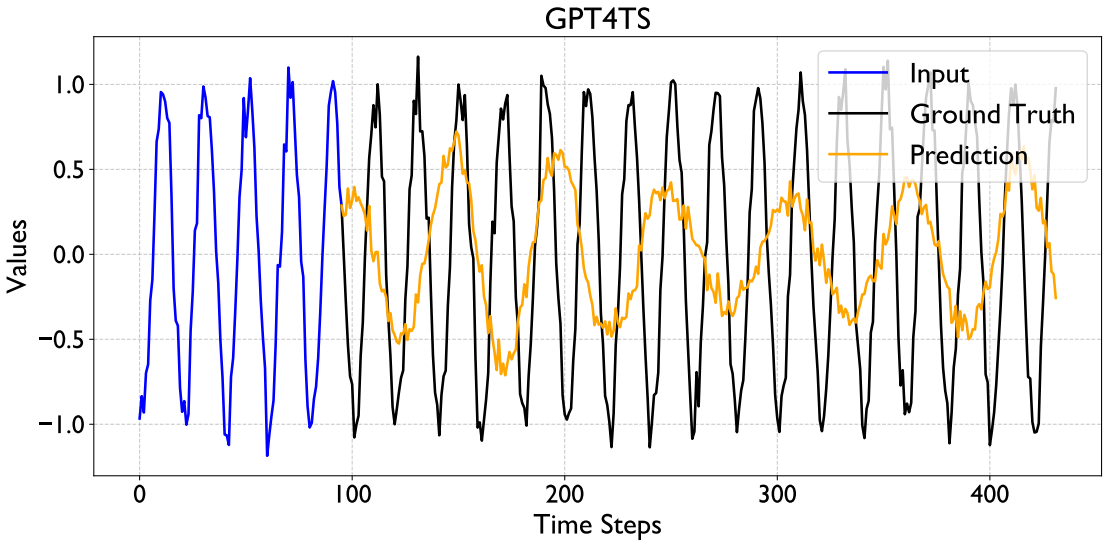

Figure 7: GPT4TS on synthetic data

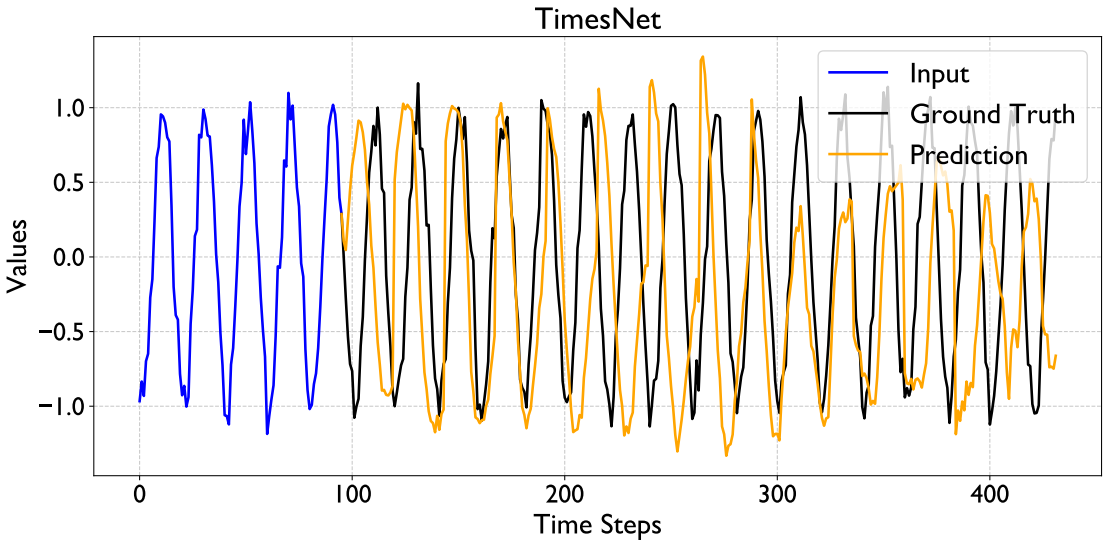

Figure 8: TimesNet on synthetic data

where $w_1 = 0.1$, $w_2 = 0.2$, $w_3 = 0.3$, $w_4 = 0.4$; $f_1 = \frac{1}{40}$, $f_2 = \frac{1}{45}$, $f_3 = \frac{1}{50}$, $f_4 = \frac{1}{55}$; $p_1 = 0$, $p_2 = 1$, $p_3 = 2$, $p_4 = 3$; and $\epsilon = 0.1$ is the noise level. We generated a long sequence of length $10,000$ and then sampled a batch of size 64 with a sequence length of 96 and a prediction length of 336 to train GPT4TS, TimesNet, and LLM-TS on this data for $1,000$ iterations. For testing, we created a test set with frequency $f = \frac{1}{20}$, which is greater than $\max(f_1, f_2, f_3, f_4)$, and used $p = 2.5$, $w = 1$ and $\epsilon = 0.1$.

As shown in Figure 7, Figure 8 an Figure 9, we can know:

- GPT4TS fails to accurately capture periodic information as it relies solely on a language model without incorporating traditional mathematical modelling.
- TimesNet generally captures periodic information due to the use of the FFT mathematical operator, but it still does not perfectly match the ground truth.

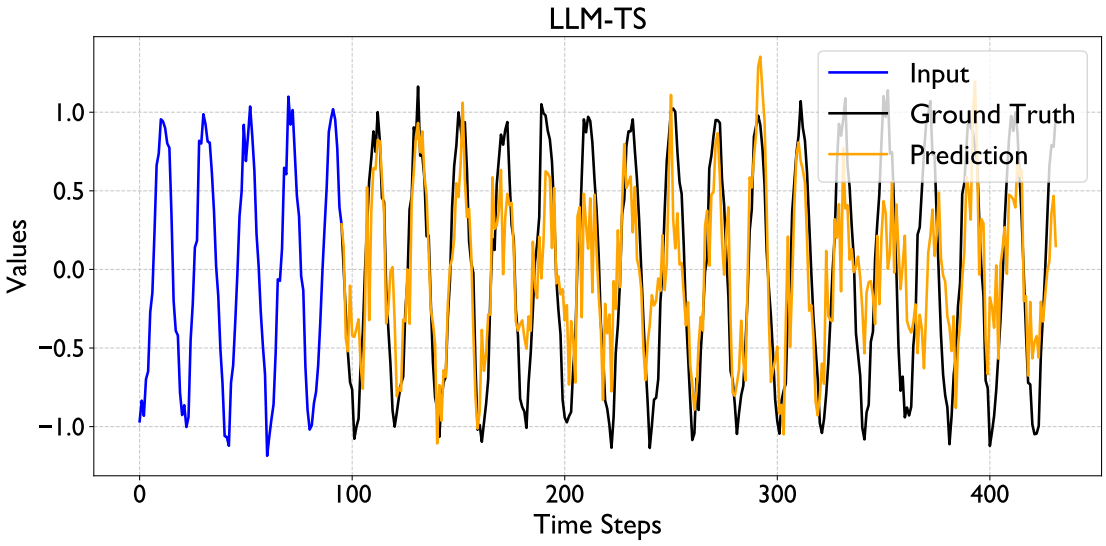

Figure 9: LLM-TS on synthetic data

- LLM-TS captures periodic information and better matches the ground truth by integrating rich language model insights into the traditional TimesNet model.

This case study highlights how the LLM-TS Integrator framework benefits from both inherent properties of traditional TS models and pattern recognition abilities of LLMs, demonstrating the effectiveness of our approach.

A.5 Template Variation

We conducted additional experiments on the ETTh1 dataset for long-term forecasting with GPT2. The original template achieves a Mean Squared Error (MSE) of 0.464 and a Mean Absolute Error (MAE) of 0.458. We tested variations of the template by changing the original context from "The Electricity Transformer Temperature is a crucial indicator in electric power long-term deployment." to:

- Variation 1: "The temperature of the electricity transformer is a vital metric for long-term electric power deployment."
- Variation 2: "Monitoring the temperature of electricity transformers is essential for the long-term deployment of electric power."
- Variation 3: "The temperature of electricity transformers serves as a key indicator in the long-term deployment of electric power."
- Variation 4: No template.

Besides, we also consider the following changes:

- w/o Input Statistics: excluding input statistical data from our analysis.
- w/o Mean, Max, Median: remove mean, max and median informatino.
- w/o Lags: remove lags information.

The performance of these variations is summarized in Table 9. These results indicate that the performance is quite similar across different variations, supporting the robustness of our approach regardless of minor

template modifications. For further details on the template implementation, refer to our code repository at `https://anonymous.4open.science/r/llm_ts_anonymous-F07D/utils/tools.py`.

Table 9: Performance across different template variations (standard error)

Template Variation	MSE	MAE
Original Template	0.464 ± 0.002	0.458 ± 0.003
Variation 1	0.460 ± 0.003	0.456 ± 0.002
Variation 2	0.465 ± 0.003	0.460 ± 0.003
Variation 3	0.464 ± 0.002	0.459 ± 0.002
Variation 4 (No template)	0.466 ± 0.003	0.460 ± 0.003
w/o Input Statistics	0.468 ± 0.002	0.462 ± 0.002
w/o Mean/Max/Median	0.465 ± 0.002	0.459 ± 0.002
w/o Lags	0.467 ± 0.002	0.460 ± 0.003

A.6 Model Efficiency Analysis

Compared to TimesNet, our *LLM-TS integrator* introduces additional costs due to the mutual information and sample weighting modules. However, after training, the inference cost of our method is the same as TimesNet. We detail the time cost of each component for ETTh1 and ETTm1 tasks, using a batch size of 32 on a 32G V100 GPU. As shown in Table 10, the training cost of our method is reasonable, given that it achieves the best performance across most tasks.

It is important to note that we use the pre-trained LLM to obtain the text embeddings only once. These embeddings can then be used throughout the training process. For instance, obtaining the embeddings for the ETTh1 dataset using the llama-3b model on an A100 GPU takes approximately 1 hour. We acknowledge that embedding extraction may become more time-consuming and memory-intensive with significantly larger or multivariate datasets. In such scenarios, strategies such as prioritizing difficult or representative data points could be employed to manage computational costs effectively. After this, the embeddings are utilized in our framework to train the model, and in the final output of the TimesNet model. This ensures that the inference time of our method is identical to that of the TimesNet model.

As detailed in the TimesNet paper, our backbone model TimesNet is relatively small with 0.067 MB parameters. For comparison, other models have the following sizes: Non-stationary Transformer has 1.884 MB, Autoformer has 1.848 MB, FEDformer has 2.9 MB, LightTS has 0.163 MB, DLinear has 0.296 MB, ETSformer has 1.123 MB, Informer has 1.903 MB, Reformer has 1.157 MB, and Pyraformer has 1.308 MB. The introduced mutual information network consists of only two linear layers of size $64x64$ and $64x4096$, which is negligible in terms of additional parameters. Similarly, the introduced MLP network consists of four layers: 1×100, 100×1, 1×1, and 1×1, and the number of parameters is also negligible.

Thus, our model remains very small and efficient, with inference time identical to TimesNet (as the mutual information component is only used during training). Given that many TS models are primarily used for inference, our approach offers effective performance gains with minimal additional computational cost.

From a theoretical standpoint, let d_α denote the dimension of the weighting network parameters and d_θ denote the dimension of the prediction network parameters. Denote the computation cost of Eq. (6) as $c(d_\alpha, d_\theta)$. According to Section 4 of Franceschi et al. (2017), the time complexity of the bi-level optimization is $O(c(d_\alpha, d_\theta))$, with the primary computational cost arising from the Jacobian-vector product in Eq. (7). This explains the time complexity of the sample reweighting module.

A.7 Full Results of Short-term Forecasting

Table 11 displays the comprehensive results for short-term forecasting.

Table 10: Cost Comparison per step(s).

Methods	Overall	TimesNet	Mutual Information	Sample Reweighting
ETTh1	3.177	0.126	0.577	2.474
Weather	5.563	0.436	1.094	4.033

Table 11: Full results of short-term forecasting.

Methods		LLM-TS	TimesNet	GPT4TS	TIME-LLM	PatchTST	N-HiTS	N-BEATS	FEDformer	Stationary	Autoformer
Yearly	*SMAPE*	13.369	13.512	13.531	13.419	13.477	13.418	13.436	13.728	13.717	13.974
	MASE	3.021	3.065	3.015	3.0050	3.019	3.045	3.043	3.048	3.078	3.134
	OWA	0.789	0.799	0.793	0.789	0.792	0.793	0.794	0.803	0.807	0.822
Quarterly	*SMAPE*	10.020	10.069	10.177	10.110	10.38	10.202	10.124	10.792	10.958	11.338
	MASE	1.162	1.178	1.194	1.178	1.233	1.194	1.169	1.283	1.325	1.365
	OWA	0.878	0.887	0.898	0.889	0.921	0.899	0.886	0.958	0.981	1.012
Monthly	*SMAPE*	12.696	12.783	12.894	12.980	12.959	12.791	12.677	14.260	13.917	13.958
	MASE	0.936	0.949	0.956	0.963	0.970	0.969	0.937	1.102	1.097	1.103
	OWA	0.880	0.889	0.897	0.903	0.905	0.899	0.880	1.012	0.998	1.002
Others	*SMAPE*	4.916	4.954	4.940	4.795	4.952	5.061	4.925	4.954	6.302	5.485
	MASE	3.310	3.364	3.228	3.178	3.347	3.216	3.391	3.264	4.064	3.865
	OWA	1.039	1.052	1.029	1.006	1.049	1.040	1.053	1.036	1.304	1.187
Average	*SMAPE*	11.819	11.908	11.991	11.983	12.059	11.927	11.851	12.840	12.780	12.909
	MASE	1.588	1.612	1.600	1.595	1.623	1.613	1.599	1.701	1.756	1.771
	OWA	0.851	0.860	0.861	0.859	0.869	0.861	0.855	0.918	0.930	0.939

A.8 Full Results of Long-Term Forecasting

Full results for long-term forecasting are presented in Table 12.

A.9 Full Results of Imputation.

Table 13 contains the detailed results of our imputation tasks.

A.10 Full Results of Classification

Table 14 contains the comprehensive results for classification.

A.11 Full Results of Anamoly Detection

Full results for anamoly detection are detailed in Table 15.

A.12 Further Ablation Studies

MLP. Given that our template comprises only simple summary statistics of the time series and the original values, we investigated whether the LLM component is essential. To this end, we replaced the LLM with an MLP that accepts the normalized concatenated statistics (mean, max, median, lags) and outputs an embedding of identical dimension to the LLM. We conducted experiments on ETTh1 and ETTm1. For ETTm1, the MSE increased from 0.401 to 0.420, and the MAE increased from 0.409 to 0.425. Similarly, for ETTh1, the MSE increased from 0.454 to 0.478, and the MAE increased from 0.451 to 0.463. These results demonstrate that the LLM component is crucial in effectively capturing the mutual information from the template, thereby justifying its use in our approach. Tan et al. (2024) demonstrate that using LLMs as prediction backbones may not yield substantial improvements; however, our results highlight the effectiveness of LLM embeddings when integrated as auxiliary information within traditional time-series models.

Table 12: Full results for long-term forecasting. We use prediction length $O \in \{96, 192, 336, 720\}$ except for ILI and $O \in \{24, 36, 48, 60\}$ for ILI. A lower MSE indicates better performance.

Methods		LLM-TS		TimesNet		TIME-LLM		DLinear		PatchTST		GPT4TS		FEDformer		TEST		Stationary		ETSformer	
Metric		MSE	MAE	MSE	MAE	MSE	MAE	MSE	MAE	MSE	MAE	MSE	MAE	MSE	MAE	MSE	MAE	MSE	MAE	MSE	MAE
Weather	96	0.166	0.217	0.174	0.224	0.202	0.239	0.196	0.255	0.186	0.227	0.196	0.234	0.217	0.296	0.214	0.264	0.173	0.223	0.197	0.281
	192	0.229	0.269	0.235	0.272	0.245	0.277	0.237	0.296	0.234	0.265	0.241	0.271	0.276	0.336	0.262	0.298	0.245	0.285	0.237	0.312
	336	0.278	0.302	0.235	0.272	0.300	0.313	0.283	0.335	0.284	0.301	0.296	0.308	0.339	0.380	0.310	0.329	0.321	0.338	0.298	0.353
	720	0.354	0.351	0.365	0.358	0.369	0.356	0.345	0.381	0.356	0.349	0.367	0.354	0.403	0.428	0.378	0.370	0.414	0.410	0.352	0.288
	Avg	0.257	0.285	0.265	0.290	0.279	0.296	0.265	0.317	0.265	0.285	0.275	0.292	0.309	0.360	0.291	0.315	0.288	0.314	0.271	0.334
ETTh1	96	0.403	0.420	0.414	0.431	0.414	0.422	0.386	0.400	0.460	0.447	0.409	0.415	0.376	0.419	0.411	0.426	0.513	0.491	0.494	0.479
	192	0.440	0.441	0.463	0.456	0.466	0.450	0.437	0.432	0.512	0.477	0.468	0.446	0.420	0.448	0.475	0.461	0.534	0.504	0.538	0.504
	336	0.471	0.457	0.487	0.466	0.515	0.475	0.481	0.459	0.546	0.496	0.503	0.461	0.459	0.465	0.508	0.482	0.588	0.535	0.574	0.521
	720	0.503	0.487	0.517	0.494	0.503	0.487	0.519	0.516	0.544	0.517	0.510	0.482	0.506	0.507	0.504	0.494	0.643	0.616	0.562	0.535
	Avg	0.454	0.451	0.470	0.462	0.474	0.459	0.456	0.452	0.516	0.484	0.473	0.451	0.440	0.460	0.475	0.466	0.570	0.537	0.542	0.510
ETTh2	96	0.322	0.366	0.340	0.374	0.306	0.353	0.333	0.387	0.308	0.355	0.298	0.350	0.358	0.397	0.328	0.374	0.476	0.458	0.340	0.391
	192	0.400	0.409	0.399	0.410	0.386	0.399	0.477	0.476	0.393	0.405	0.376	0.399	0.429	0.439	0.403	0.418	0.512	0.493	0.430	0.439
	336	0.432	0.435	0.452	0.452	0.460	0.458	0.594	0.541	0.427	0.436	0.430	0.439	0.496	0.487	0.455	0.458	0.552	0.551	0.485	0.479
	720	0.430	0.442	0.462	0.468	0.442	0.451	0.831	0.657	0.436	0.450	0.428	0.451	0.463	0.474	0.470	0.477	0.562	0.560	0.500	0.497
	Avg	0.396	0.413	0.413	0.426	0.398	0.415	0.559	0.515	0.391	0.411	0.383	0.410	0.437	0.449	0.414	0.432	0.526	0.516	0.439	0.452
ETTm1	96	0.329	0.371	0.340	0.377	0.393	0.398	0.345	0.372	0.352	0.374	0.350	0.369	0.379	0.419	0.336	0.373	0.386	0.398	0.375	0.398
	192	0.380	0.398	0.406	0.408	0.412	0.405	0.380	0.389	0.390	0.393	0.387	0.387	0.426	0.441	0.381	0.399	0.459	0.444	0.408	0.410
	336	0.418	0.425	0.424	0.425	0.442	0.425	0.413	0.413	0.421	0.414	0.418	0.407	0.445	0.459	0.411	0.418	0.495	0.464	0.435	0.428
	720	0.476	0.440	0.485	0.461	0.502	0.457	0.474	0.453	0.462	0.449	0.477	0.437	0.543	0.490	0.478	0.454	0.585	0.516	0.499	0.462
	Avg	0.401	0.409	0.414	0.418	0.437	0.421	0.403	0.407	0.406	0.407	0.408	0.400	0.448	0.452	0.402	0.411	0.481	0.456	0.429	0.425
ETTm2	96	0.189	0.266	0.185	0.264	0.193	0.281	0.193	0.292	0.183	0.270	0.185	0.271	0.203	0.287	0.230	0.307	0.192	0.274	0.189	0.280
	192	0.253	0.307	0.252	0.306	0.254	0.315	0.284	0.363	0.255	0.314	0.250	0.312	0.269	0.328	0.284	0.338	0.280	0.339	0.253	0.319
	336	0.315	0.345	0.323	0.350	0.320	0.355	0.369	0.427	0.309	0.347	0.314	0.351	0.325	0.366	0.340	0.370	0.334	0.361	0.314	0.357
	720	0.421	0.408	0.415	0.403	0.426	0.416	0.554	0.522	0.412	0.404	0.410	0.408	0.421	0.415	0.436	0.420	0.417	0.413	0.414	0.413
	Avg	0.295	0.331	0.294	0.331	0.298	0.342	0.350	0.401	0.290	0.334	0.290	0.335	0.305	0.349	0.323	0.359	0.306	0.347	0.293	0.342
ILI	24	1.921	0.898	2.072	0.948	2.589	1.054	2.398	1.040	2.229	0.894	5.259	1.689	3.228	1.260	3.371	1.231	2.294	0.945	2.527	1.020
	36	2.151	0.933	2.494	1.019	2.996	1.194	2.646	1.088	2.330	0.925	6.136	1.831	2.679	1.080	3.725	1.322	1.825	0.848	2.615	1.007
	48	2.062	0.892	2.298	0.964	2.714	1.095	2.614	1.086	2.140	0.894	4.670	1.562	2.622	1.078	3.291	1.237	2.010	0.900	2.359	0.972
	60	1.759	0.853	2.198	0.963	2.605	1.050	2.804	1.146	2.037	0.912	4.402	1.517	2.857	1.157	2.907	1.136	2.178	0.963	2.487	1.016
	Avg	1.973	0.894	2.266	0.974	2.726	1.098	2.616	1.090	2.184	0.906	5.117	1.650	2.847	1.144	3.324	1.232	2.077	0.914	2.497	1.004
ECL	96	0.167	0.271	0.169	0.273	0.207	0.292	0.197	0.282	0.190	0.296	0.186	0.273	0.193	0.308	0.218	0.309	0.169	0.273	0.187	0.304
	192	0.178	0.280	0.186	0.288	0.209	0.297	0.196	0.285	0.199	0.304	0.190	0.278	0.201	0.315	0.220	0.311	0.182	0.286	0.199	0.315
	336	0.198	0.302	0.206	0.305	0.224	0.312	0.209	0.301	0.217	0.319	0.204	0.291	0.214	0.329	0.234	0.323	0.200	0.304	0.212	0.329
	720	0.233	0.344	0.231	0.327	0.277	0.359	0.245	0.333	0.258	0.352	0.245	0.297	0.325	0.355	0.276	0.354	0.222	0.321	0.233	0.345
	Avg	0.194	0.299	0.198	0.298	0.229	0.315	0.212	0.300	0.216	0.318	0.206	0.285	0.214	0.327	0.237	0.324	0.193	0.296	0.208	0.323
Traffic	96	0.587	0.315	0.589	0.313	0.609	0.402	0.650	0.396	0.526	0.347	0.563	0.378	0.587	0.366	0.589	0.390	0.612	0.338	0.607	0.392
	192	0.612	0.326	0.627	0.337	0.586	0.382	0.598	0.370	0.522	0.332	0.549	0.367	0.604	0.373	0.567	0.380	0.613	0.340	0.621	0.399
	336	0.634	0.338	0.635	0.341	0.593	0.390	0.605	0.373	0.517	0.334	0.566	0.376	0.621	0.383	0.583	0.389	0.618	0.328	0.622	0.396
	720	0.640	0.351	0.658	0.349	0.636	0.405	0.645	0.394	0.552	0.352	0.567	0.372	0.626	0.382	0.585	0.391	0.653	0.355	0.632	0.396
	Avg	0.618	0.333	0.627	0.335	0.606	0.395	0.625	0.383	0.529	0.341	0.561	0.373	0.610	0.376	0.581	0.388	0.624	0.340	0.621	0.396
Average		0.574	0.427	0.618	0.442	0.681	0.468	0.686	0.483	0.600	0.436	0.964	0.525	0.701	0.489	0.756	0.491	0.633	0.465	0.662	0.473

Mutual Information Estimator. In the main paper, we utilize the Jensen-Shannon mutual information (MI) estimator. Additionally, we explore the Mutual Information Neural Estimator (MINE) (Hjelm et al., 2019a). We evaluate both estimators on two tasks, ETTh1 and ETTm1, with results averaged over four prediction lengths. For ETTh1, the MSE and MAE using the original Jensen-Shannon estimator are 0.454 and 0.451, respectively, compared to 0.460 and 0.457 with MINE. For ETTm1, the MSE and MAE are 0.401 and 0.409 with the original estimator, and 0.402 and 0.410 with MINE. These comparisons highlight the robustness of our method across different mutual information estimators.

Sample Reweighting Illustration. Figures 11, 10, 12, and 13 display the learned weighting network applied to various datasets: MSL for anomaly detection, Weather for forecasting, ETTh1 for imputation, and PEMS-SF for classification. These visualizations corroborate our hypothesis: the sample weight ω_O increases with the prediction loss l_O, while the weight ω_I decreases as l_O increases. This observed pattern supports the efficacy of our reweighting strategy.

Static Weighting Scheme. We also explore a static weighting scheme as a contrast to the dynamic weighting used in our sample reweighting module. This scheme balances the prediction loss and mutual information loss, with a ratio of 0.0 representing pure prediction loss and 1.0 representing pure mutual

Table 13: Full results for the imputation task. Randomly masked {12.5%, 25%, 37.5%, 50%} of points in 96-length series, averaging results over 4 mask ratios.

Methods		LLM-TS		TimesNet		GPT4TS		PatchTST		LightTS		DLinear		FEDformer		Stationary		Autoformer		Reformer	
Mask	Ratio	MSE	MAE	MSE	MAE	MSE	MAE	MSE	MAE	MSE	MAE	MSE	MAE	MSE	MAE	MSE	MAE	MSE	MAE	MSE	MAE
ETTm1	12.5%	0.018	0.088	0.023	0.101	0.018	0.089	0.041	0.130	0.093	0.206	0.080	0.193	0.052	0.166	0.032	0.119	0.046	0.144	0.042	0.146
	25%	0.022	0.097	0.023	0.101	0.023	0.099	0.044	0.135	0.093	0.206	0.080	0.193	0.052	0.166	0.032	0.119	0.046	0.144	0.042	0.146
	37.5%	0.027	0.108	0.029	0.112	0.030	0.112	0.049	0.143	0.113	0.231	0.103	0.219	0.069	0.191	0.039	0.131	0.057	0.161	0.063	0.182
	50%	0.033	0.120	0.035	0.123	0.042	0.131	0.055	0.151	0.134	0.255	0.132	0.248	0.089	0.218	0.047	0.145	0.067	0.174	0.082	0.208
	Avg	0.025	0.103	0.028	0.109	0.028	0.108	0.047	0.140	0.104	0.218	0.093	0.206	0.062	0.177	0.036	0.126	0.051	0.150	0.055	0.166
ETTm2	12.5%	0.018	0.079	0.019	0.081	0.019	0.078	0.108	0.239	0.034	0.127	0.062	0.166	0.056	0.159	0.021	0.088	0.023	0.092	0.108	0.228
	25%	0.020	0.085	0.021	0.087	0.021	0.084	0.028	0.099	0.042	0.143	0.085	0.196	0.080	0.195	0.024	0.096	0.026	0.101	0.136	0.262
	37.5%	0.022	0.089	0.023	0.092	0.024	0.090	0.030	0.104	0.051	0.159	0.106	0.222	0.110	0.231	0.027	0.103	0.030	0.108	0.175	0.300
	50%	0.025	0.096	0.025	0.097	0.027	0.098	0.034	0.110	0.059	0.174	0.131	0.247	0.156	0.276	0.030	0.108	0.035	0.119	0.211	0.329
	Avg	0.021	0.087	0.022	0.089	0.023	0.088	0.029	0.102	0.046	0.151	0.096	0.208	0.101	0.215	0.026	0.099	0.029	0.105	0.157	0.280
ETTh1	12.5%	0.058	0.165	0.064	0.170	0.043	0.141	0.093	0.201	0.240	0.345	0.151	0.267	0.070	0.190	0.060	0.165	0.074	0.182	0.074	0.194
	25%	0.077	0.189	0.082	0.192	0.056	0.159	0.107	0.217	0.265	0.364	0.180	0.292	0.106	0.236	0.080	0.189	0.090	0.203	0.102	0.227
	37.5%	0.096	0.209	0.098	0.209	0.074	0.182	0.120	0.230	0.296	0.382	0.215	0.318	0.124	0.258	0.102	0.212	0.109	0.222	0.135	0.261
	50%	0.118	0.228	0.116	0.226	0.104	0.214	0.141	0.248	0.334	0.404	0.257	0.347	0.165	0.299	0.133	0.240	0.137	0.248	0.179	0.298
	Avg	0.087	0.198	0.090	0.199	0.069	0.174	0.115	0.224	0.284	0.373	0.201	0.306	0.117	0.246	0.094	0.201	0.103	0.214	0.122	0.245
ETTh2	12.5%	0.039	0.131	0.040	0.132	0.041	0.129	0.057	0.152	0.101	0.231	0.100	0.216	0.095	0.212	0.042	0.133	0.044	0.138	0.163	0.289
	25%	0.046	0.143	0.048	0.146	0.046	0.137	0.061	0.158	0.115	0.246	0.127	0.247	0.137	0.258	0.049	0.147	0.050	0.149	0.206	0.331
	37.5%	0.053	0.154	0.055	0.156	0.053	0.148	0.067	0.166	0.126	0.257	0.158	0.276	0.187	0.304	0.056	0.158	0.060	0.163	0.252	0.370
	50%	0.061	0.165	0.061	0.165	0.060	0.160	0.073	0.174	0.136	0.268	0.183	0.299	0.232	0.341	0.065	0.170	0.068	0.173	0.316	0.419
	Avg	0.050	0.148	0.051	0.150	0.050	0.144	0.065	0.163	0.119	0.250	0.142	0.259	0.163	0.279	0.053	0.152	0.055	0.156	0.234	0.352
ECL	12.5%	0.087	0.203	0.090	0.204	0.080	0.194	0.055	0.160	0.102	0.229	0.092	0.214	0.107	0.237	0.093	0.210	0.089	0.210	0.190	0.308
	25%	0.091	0.207	0.092	0.209	0.087	0.203	0.065	0.175	0.121	0.252	0.118	0.247	0.120	0.251	0.097	0.214	0.096	0.220	0.197	0.312
	37.5%	0.095	0.213	0.096	0.213	0.094	0.211	0.076	0.344	0.141	0.273	0.144	0.276	0.136	0.266	0.102	0.220	0.104	0.229	0.203	0.315
	50%	0.101	0.220	0.102	0.221	0.101	0.220	0.091	0.208	0.160	0.293	0.175	0.305	0.158	0.284	0.108	0.228	0.113	0.239	0.210	0.319
	Avg	0.094	0.211	0.095	0.212	0.091	0.207	0.072	0.183	0.131	0.262	0.132	0.260	0.130	0.259	0.100	0.218	0.101	0.225	0.200	0.313
Weather	12.5%	0.026	0.048	0.025	0.047	0.027	0.049	0.029	0.049	0.047	0.101	0.039	0.084	0.041	0.107	0.027	0.051	0.026	0.047	0.031	0.076
	25%	0.029	0.055	0.031	0.062	0.030	0.054	0.031	0.053	0.052	0.111	0.048	0.103	0.064	0.163	0.029	0.056	0.030	0.054	0.035	0.082
	37.5%	0.032	0.059	0.034	0.064	0.034	0.062	0.035	0.058	0.058	0.121	0.057	0.117	0.107	0.229	0.033	0.062	0.032	0.060	0.040	0.091
	50%	0.033	0.061	0.035	0.062	0.037	0.066	0.038	0.063	0.065	0.133	0.066	0.134	0.183	0.312	0.037	0.068	0.037	0.067	0.046	0.099
	Avg	0.030	0.056	0.031	0.059	0.032	0.058	0.060	0.144	0.055	0.117	0.052	0.110	0.099	0.203	0.032	0.059	0.031	0.057	0.038	0.087

Table 14: Complete classification task results. $*$. in the Transformers indicates the name of $*$former.

Methods	Classical		RNN		TCN	Transformers									MLP		TimesNet	LLM		LLM-TS
	XGB	Roc	LSTNet	LSSL		Trans.	Re.	In.	Pyra.	Auto.	Station.	FED.	ETS.	Flow.	DL	LTS.		GPT4TS	TEST	
Ethanol	43.7	45.2	39.9	31.1	28.9	32.7	31.9	31.6	30.8	31.6	32.7	31.2	28.1	33.8	32.6	29.7	30.4	26.2	25.1	31.9
FaceD	63.3	64.7	65.7	66.7	52.8	67.3	68.6	67.0	65.7	68.4	68.0	66.0	66.3	67.6	68.0	67.5	68.6	67.8	50.1	68.9
HandW	15.8	58.8	25.8	24.6	53.3	32.0	27.4	32.8	29.4	36.7	31.6	28.0	32.5	33.8	27.0	26.1	32.1	28.9	20.1	32.7
HeartB	73.2	75.6	77.1	72.7	75.6	76.1	77.1	80.5	75.6	74.6	73.7	73.7	71.2	77.6	75.1	75.1	77.6	72.2	73.7	77.1
JapanV	86.5	96.2	98.1	98.4	98.9	98.7	97.8	98.9	98.4	96.2	99.2	98.4	95.9	98.9	96.2	96.2	97.2	98.4	78.4	98.1
PEMS	98.3	75.1	86.7	86.1	68.8	82.1	82.7	81.5	83.2	82.7	87.3	80.9	86.0	83.8	75.1	88.4	89.6	79.2	59.5	90.8
SCP1	84.6	90.8	84.0	90.8	84.6	92.2	90.4	90.1	88.1	84.0	89.4	88.7	89.6	92.5	87.3	89.8	90.4	90.1	84.0	91.8
SCP2	48.9	53.3	52.8	52.2	55.6	53.9	56.7	53.3	53.3	50.6	57.2	54.4	55.0	56.1	50.5	51.1	57.1	50.0	54.4	57.8
SpokenA	69.6	71.2	100.0	100.0	95.6	98.4	97.0	100.0	99.6	100.0	100.0	100.0	100.0	98.8	81.4	100.0	98.6	97.9	82.1	98.6
UWave	75.9	94.4	87.8	85.9	88.4	85.6	85.6	85.6	83.4	85.9	87.5	85.3	85.0	86.6	82.1	80.3	85.5	85.6	84.4	86.6
Avg	66.0	72.5	71.8	70.9	70.3	71.9	71.5	72.1	70.8	71.1	72.7	70.7	71.0	73.0	67.5	70.4	72.7	69.5	61.2	**73.4**

information loss. As shown in Table 18, the static approach underperforms relative to our dynamic sample weighting module, demonstrating the superior effectiveness of our method.

A.12.1 Comprehensive Results.

The detailed performance of various traditional TS models and LLMs is presented in Table 16 and Table 17.

Table 15: Full results for the anomaly detection.

Methods	SMD			MSL			SMAP			SWaT			PSM			Avg F1
Metrics	P	R	F1	P	R	F1	P	R	F1	P	R	F1	P	R	F1	%
LLM-TS	88.09	81.54	84.69	89.04	74.49	81.11	89.95	56.51	69.41	91.16	95.40	93.23	98.44	96.45	97.43	85.17
TimesNet	87.93	81.45	84.57	88.62	73.48	80.34	89.59	56.35	69.18	91.00	95.33	93.12	98.40	96.18	97.27	84.90
GPT4TS	87.70	81.19	84.32	82.15	81.32	81.73	90.04	55.75	68.86	92.12	93.06	92.59	98.37	96.34	97.34	84.97
PatchTST	87.26	82.14	84.62	88.34	70.96	78.70	90.64	55.46	68.82	91.10	80.94	85.72	98.84	93.47	96.08	82.79
ETSformer	87.44	79.23	83.13	85.13	84.93	85.03	92.25	55.75	69.50	90.02	80.36	84.91	99.31	85.28	91.76	82.87
FEDformer	87.95	82.39	85.08	77.14	80.07	78.57	90.47	58.10	70.76	90.17	96.42	93.19	97.31	97.16	97.23	84.97
LightTS	87.10	78.42	82.53	82.40	75.78	78.95	92.58	55.27	69.21	91.98	94.72	93.33	98.37	95.97	97.15	84.23
DLinear	83.62	71.52	77.10	84.34	85.42	84.88	92.32	55.41	69.26	80.91	95.30	87.52	98.28	89.26	93.55	82.46
Stationary	88.33	81.21	84.62	68.55	89.14	77.50	89.37	59.02	71.09	68.03	96.75	79.88	97.82	96.76	97.29	82.08
Autoformer	88.06	82.35	85.11	77.27	80.92	79.05	90.40	58.62	71.12	89.85	95.81	92.74	99.08	88.15	93.29	84.26
Pyraformer	85.61	80.61	83.04	83.81	85.93	84.86	92.54	57.71	71.09	87.92	96.00	91.78	71.67	96.02	82.08	82.57
Anomaly Transformer	88.91	82.23	85.49	79.61	87.37	83.31	91.85	58.11	71.18	72.51	97.32	83.10	68.35	94.72	79.40	80.50
Informer	86.60	77.23	81.65	81.77	86.48	84.06	90.11	57.13	69.92	70.29	96.75	81.43	64.27	96.33	77.10	78.83
Reformer	82.58	69.24	75.32	85.51	83.31	84.40	90.91	57.44	70.40	72.50	96.53	82.80	59.93	95.38	73.61	77.31
Transformer	83.58	76.13	79.56	71.57	87.37	78.68	89.37	57.12	69.70	68.84	96.53	80.37	62.75	96.56	76.07	76.88

Table 16: Different traditional models. We use prediction length $O \in \{96, 192, 336, 720\}$ for ILI and $O \in \{24, 36, 48, 60\}$ for others.

Methods		PatchTST		PatchTST INT		ETSformer		ETS INT		Stationary		Stat INT		FreTS		FreTS INT	
Metric		MSE	MAE	MSE	MAE	MSE	MAE	MSE	MAE	MSE	MAE	MSE	MAE	MSE	MAE	MSE	MAE
Weather	96	0.174	0.216	0.172	0.214	0.196	0.282	0.200	0.285	0.178	0.226	0.201	0.246	0.187	0.243	0.179	0.235
	192	0.222	0.258	0.219	0.255	0.282	0.364	0.278	0.361	0.235	0.278	0.238	0.280	0.227	0.274	0.221	0.278
	336	0.280	0.298	0.279	0.298	0.344	0.409	0.322	0.382	0.327	0.339	0.312	0.329	0.281	0.325	0.276	0.320
	720	0.356	0.349	0.356	0.348	0.430	0.472	0.427	0.470	0.387	0.383	0.386	0.383	0.352	0.382	0.344	0.376
	Avg	0.258	0.280	0.257	0.279	0.313	0.382	0.307	0.375	0.282	0.307	0.284	0.309	0.262	0.306	0.255	0.302
ETTh1	96	0.381	0.398	0.382	0.401	0.554	0.536	0.550	0.532	0.534	0.499	0.523	0.486	0.398	0.412	0.395	0.409
	192	0.421	0.426	0.422	0.428	0.686	0.619	0.690	0.621	0.639	0.560	0.609	0.560	0.454	0.449	0.455	0.451
	336	0.464	0.449	0.460	0.441	0.869	0.730	0.868	0.728	0.790	0.648	0.780	0.634	0.512	0.483	0.502	0.474
	720	0.527	0.500	0.510	0.496	1.085	0.849	1.054	0.830	0.706	0.620	0.701	0.606	0.572	0.547	0.560	0.530
	Avg	0.448	0.443	0.444	0.442	0.799	0.684	0.791	0.678	0.667	0.582	0.653	0.572	0.484	0.473	0.478	0.466
ETTm1	96	0.332	0.368	0.332	0.372	0.526	0.495	0.424	0.434	0.417	0.417	0.412	0.410	0.340	0.375	0.339	0.374
	192	0.368	0.388	0.367	0.388	0.565	0.538	0.458	0.461	0.446	0.437	0.445	0.435	0.395	0.408	0.384	0.399
	336	0.397	0.405	0.396	0.405	0.658	0.603	0.537	0.519	0.582	0.507	0.570	0.491	0.431	0.433	0.420	0.423
	720	0.457	0.445	0.460	0.446	0.801	0.696	0.802	0.696	0.661	0.546	0.660	0.546	0.494	0.470	0.484	0.462
	Avg	0.389	0.402	0.389	0.403	0.638	0.583	0.555	0.528	0.527	0.477	0.522	0.471	0.415	0.422	0.407	0.415
ILI	24	2.229	0.894	2.172	0.856	4.043	1.410	3.607	1.305	2.722	1.024	1.905	0.872	3.226	1.231	3.202	1.213
	36	2.330	0.925	2.347	0.978	3.809	1.358	3.705	1.315	3.026	1.071	2.790	1.068	3.363	1.259	3.000	1.173
	48	2.140	0.894	1.984	0.869	3.851	1.351	3.714	1.309	2.622	1.032	2.132	0.900	3.456	1.285	3.132	1.213
	60	2.037	0.912	1.770	0.831	3.983	1.349	3.935	1.350	2.520	1.035	1.991	0.901	3.749	1.340	3.298	1.243
	Avg	2.184	0.906	2.068	0.884	3.922	1.367	3.740	1.320	2.722	1.041	2.205	0.935	3.449	1.279	3.158	1.211

Table 17: Different LLM embeddings. We use prediction length $O \in \{96, 192, 336, 720\}$ for ILI and $O \in \{24, 36, 48, 60\}$ for others.

Methods		LLM-TS (LLaMA)		LLaMA w/o text		GPT2		BERT		No LLM	
Metric		MSE	MAE	MSE	MAE	MSE	MAE	MSE	MAE	MSE	MAE
Weather	96	0.166	0.217	0.170	0.218	0.168	0.218	0.167	0.217	0.168	0.218
	192	0.229	0.269	0.227	0.266	0.226	0.267	0.229	0.270	0.227	0.268
	336	0.278	0.302	0.295	0.314	0.292	0.310	0.283	0.305	0.298	0.318
	720	0.354	0.351	0.360	0.354	0.359	0.354	0.360	0.354	0.361	0.356
	Avg	0.257	0.285	0.263	0.288	0.261	0.287	0.260	0.287	0.264	0.290
ETTh1	96	0.403	0.420	0.409	0.427	0.408	0.426	0.402	0.421	0.402	0.422
	192	0.440	0.441	0.445	0.445	0.442	0.444	0.452	0.450	0.459	0.455
	336	0.471	0.457	0.490	0.472	0.487	0.467	0.494	0.472	0.471	0.457
	720	0.503	0.487	0.518	0.496	0.517	0.494	0.520	0.497	0.535	0.507
	Avg	0.454	0.451	0.465	0.460	0.464	0.458	0.467	0.460	0.467	0.460
ETTm1	96	0.329	0.371	0.350	0.387	0.338	0.370	0.340	0.375	0.341	0.377
	192	0.380	0.398	0.383	0.398	0.392	0.404	0.401	0.408	0.404	0.413
	336	0.418	0.425	0.423	0.426	0.416	0.423	0.414	0.421	0.432	0.428
	720	0.476	0.440	0.467	0.449	0.477	0.454	0.470	0.445	0.468	0.449
	Avg	0.401	0.409	0.406	0.415	0.406	0.413	0.406	0.412	0.411	0.417
ILI	24	1.921	0.898	1.998	0.929	1.997	0.929	1.917	0.915	2.170	0.947
	36	2.151	0.933	2.422	0.957	2.333	0.958	2.431	1.004	2.093	0.889
	48	2.062	0.892	2.198	0.964	2.269	0.937	2.333	0.961	2.418	0.959
	60	1.759	0.853	2.072	0.948	2.077	0.921	2.089	0.926	2.203	0.971
	Avg	1.973	0.894	2.173	0.950	2.169	0.936	2.193	0.952	2.221	0.942

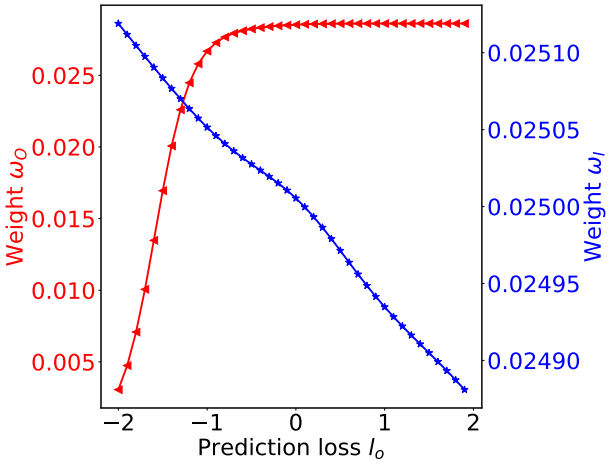

Figure 10: Forecasting.

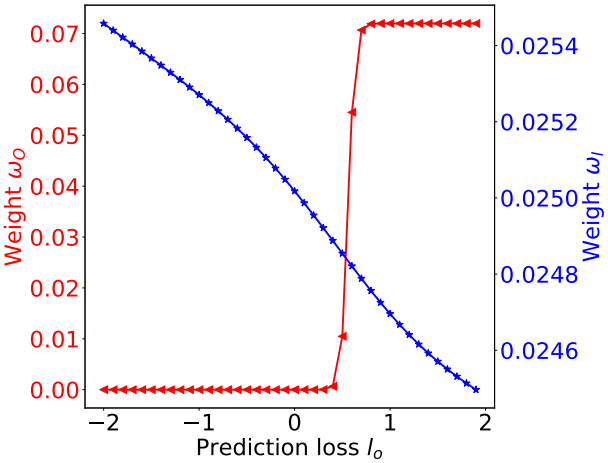

Figure 11: Anomaly detection

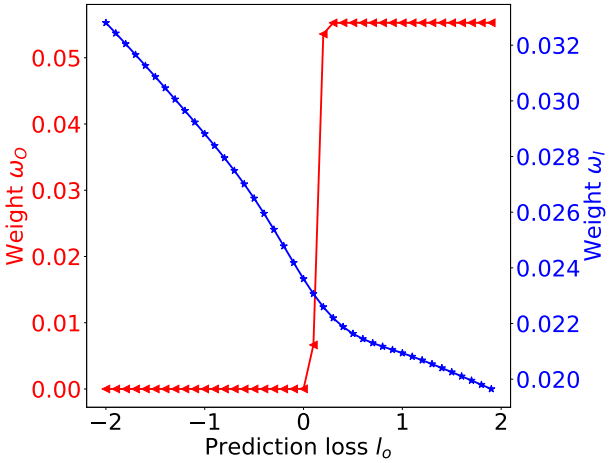

Figure 12: imputation.

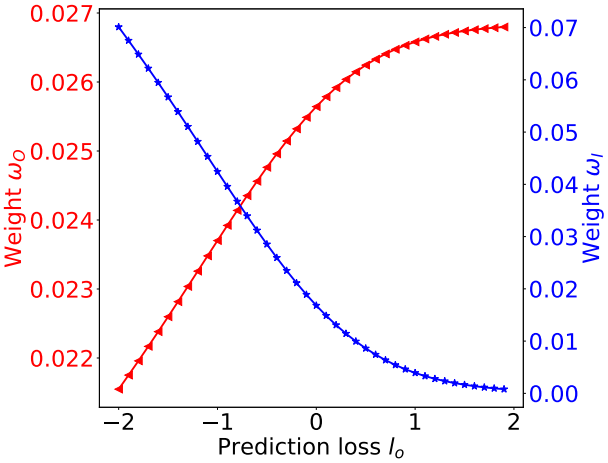

Figure 13: classification

Table 18: Static Weighting Scheme with Different ratios.

Ratio	0.0		0.2		0.4		0.6		0.8		1.0		Ours	
Metric	MSE	MAE	MSE	MAE	MSE	MAE	MSE	MAE	MSE	MAE	MSE	MAE	MSE	MAE
$ETTh1$	0.478	0.468	0.471	0.459	0.465	0.462	0.470	0.463	0.473	0.450	0.471	0.463	0.454	0.451
$ETTm1$	0.415	0.417	0.408	0.414	0.405	0.412	0.406	0.412	0.417	0.419	0.416	0.419	0.401	0.409